Materials Horizons

ROYAL SOCIETY OF CHEMISTRY

REVIEW

View Article Online
View Journal | View Issue

Cite this: *Mater. Horiz.*, 2022, 9, 1387

Three interfaces of the dental implant system and their clinical effects on hard and soft tissues

Jeong Chan Kim, [a] Min Lee [b] and In-Sung Luke Yeo *[c]

Anatomically, the human tooth has structures both embedded within and forming part of the exterior surface of the human body. When a tooth is lost, it is often replaced by a dental implant, to facilitate the chewing of food and for esthetic purposes. For successful substitution of the lost tooth, hard tissue should be integrated into the implant surface. The microtopography and chemistry of the implant surface have been explored with the aim of enhancing osseointegration. Additionally, clinical implant success is dependent on ensuring that a barrier, comprising strong gingival attachment to an abutment, does not allow the infiltration of oral bacteria into the bone-integrated surface. Epithelial and connective tissue cells respond to the abutment surface, depending on its surface characteristics and the materials from which it is made. In particular, the biomechanics of the implant–abutment connection structure (*i.e.*, the biomechanics of the interface between implant and abutment surfaces, and the screw mechanics of the implant–abutment assembly) are critical for both the soft tissue seal and hard tissue integration. Herein, we discuss the clinical importance of these three interfaces: bone–implant, gingiva–abutment, and implant–abutment.

Received 5th October 2021,
Accepted 2nd March 2022

DOI: 10.1039/d1mh01621k

rsc.li/materials-horizons

1. Introduction

An endosteal dental implant is an artificial biomedical device that is surgically installed and anchored to the jaw bone to support a supra-structure (an implant-supported prosthesis) as a replacement for missing teeth.[1] Teeth perform three main functions: mastication, speech, and esthetics (beauty), and loss of teeth can compromise these. Traditionally, dental clinicians have treated tooth loss using fixed or removable prostheses that are associated with the remaining teeth; however, with this type

[a] *Department of Periodontology, Seoul National University School of Dentistry, Seoul 03080, Korea*
[b] *Department of Bioengineering, University of California, Los Angeles, CA 90095, USA*
[c] *Department of Prosthodontics, School of Dentistry and Dental Research Institute, Seoul National University, 101 Daehak-Ro, Jongro-Gu, Seoul 03080, Korea. E-mail: pros53@snu.ac.kr; Fax: +82-2-2072-3860; Tel: +82-2-2072-2661*

Jeong Chan Kim

Jeong Chan Kim is currently a chief technical officer in an implant manufacturing company, Deep Implant System, Seongnam, Korea. He graduated from Seoul National University, Seoul, Korea, and received his master's degree in Periodontology at the same university. He is a periodontologist and was a clinical adjunct professor in the department of Periodontology at Seoul National University School of Dentistry. He is now working on the development of modified implant surfaces.

Min Lee

Min Lee is a professor in the School of Dentistry and affiliated faculty in the department of Bioengineering at the University of California, Los Angeles. He received his PhD in biomedical engineering from UCLA and joined the faculty of UCLA in 2007. Dr Lee's research focuses on the design and development of new biomaterial systems to provide fundamental bases and translational approaches to tissue engineering and regenerative medicine. Specific areas of interest are orthobiologics, material-based therapeutics to repair craniofacial and orthopedic skeletal defects, novel liposomal platform for drug and gene delivery, injectable hydrogel systems.

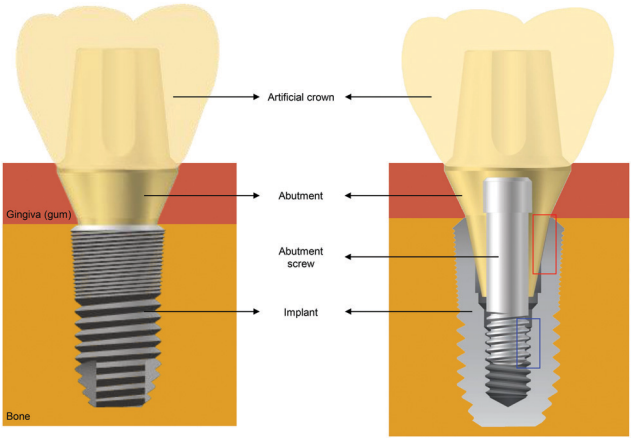

Fig. 1 Basic structure of a dental implant system. The abutment is connected to the implant by an abutment screw. In this example, the artificial crown is cemented to the abutment. The cross-sectional diagram on the right shows an implant–abutment interface, which is composed of a frictional interface between two inclined planes (red rectangle) and a screw interface (blue rectangle).

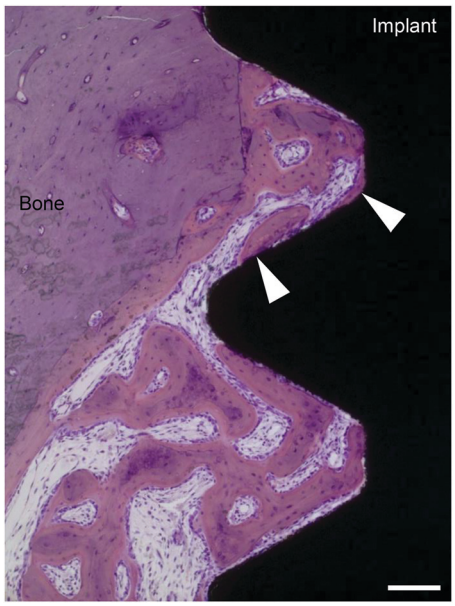

Fig. 2 Hard tissue integration (undecalcified section, stained with hematoxylin and eosin). The bone, in direct contact with the implant surface (white arrowheads), is shown in this histological image. Scale bar = 100 μm.

of prosthesis, the remaining teeth can be damaged by the various forces applied to the prosthesis.[2–4] Therefore, restoration using dental implants is preferred as a first prosthetic option, and dental implants are now the mainstream in modern clinical dentistry.

A tooth consists of a crown that projects into the oral area through the gingiva (gum) and is visible in the mouth, and a root that is submerged in the jaw bone. The structure of a dental implant system is similar to that of a tooth, where the implant is the counterpart of the root and the artificial crown is equivalent to a natural crown; however, the root and crown of a tooth form a single continuous structure, while the implant and artificial crown in an implant system are separate parts interconnected by the abutment (Fig. 1).

An implant, an abutment, and an artificial crown are the three major components of a dental implant system. As implants are placed into the jaw bone and abutments are located in the soft tissue (gingiva) area between the jaw bone and the mouth, dental implant systems have two biological interfaces: a hard tissue–implant interface and a soft tissue–abutment interface. The bone should be integrated into the implant surface to rehabilitate missing teeth, while the gingiva should be firmly attached to the abutment surface to inhibit inflammatory responses around the implant system.[5–7] The implant–abutment interface (Fig. 1) should also be considered, and its biomechanical characteristics strongly influence bone and gingiva physiology.

This review explores the interactive effects of the hard tissue–implant, soft tissue–abutment, and implant–abutment interfaces, which have not been covered in previous reviews, from a clinical perspective. In the first section, we discuss topographically or chemically modified implant surfaces affecting bone healing at the hard tissue–implant interface. In the second section, we search the clinical meaning of the soft tissue seal around abutments, discussing abutment material and design factors influencing the attachment between soft tissues and abutments. In the third section, we investigate some biomechanical formulas analyzing two typical implant–abutment connection structures, and clinically interpret material features and limitations that these formulas imply.

In-Sung Luke Yeo

In-Sung Luke Yeo is currently a professor at Seoul National University, Seoul, Korea. He served as a dental officer at Special Forces Commands in the Korean Army from the year 2003 to 2006. He completed his PhD in the department of Prosthodontics at Seoul National University School of Dentistry where his theme was on implant surface modification and bone-implant interface. He is treating patients as a prosthodontist at Seoul National University Dental Hospital, and is investigating the nature of hard and soft tissue responses to implant surfaces.

2. Bone–implant interface (hard tissue integration)

2.1. Hard tissue integration (osseointegration)

Mastication involves use of the teeth, jaw bone, and masticatory muscles, and dental implants replace the function of teeth. Therefore, implants must be strongly anchored to the jaw bone

to fulfil their masticatory role; this is referred to as hard tissue integration.[6,7] When an implant is inserted into the bone, the initial stability of the implant depends on the mechanical surface contact between the bone and the implant, referred to as 'primary stability'.[8] This physical contact can be described using the well-known mass-spring-damper model of mechanical vibration, based on the second-order differential equation, $m\frac{d^2}{dt^2}x + c\frac{d}{dt}x + kx = 0$, where m is the mass of the system, c is the damping constant, k is the spring constant, x is displacement, and t is time.[9] As the process of bone healing progresses, hard tissue integration occurs at the bone–implant interface, giving the implant secondary stability, which increases implant anchorage to the bone; this biological phenomenon complicates the mechanical interpretation of implant stability.[8,10]

Hard tissue integration, commonly called osseointegration, has been defined as 'a direct contact between a loaded implant surface and bone at the light microscopic level of resolution'[6] (Fig. 2); however, by this definition, hard tissue integration can only be observed and described using histological methods; hence the definition has been modified to be more clinically relevant. An example modified definition is 'a clinically asymptomatic rigid fixation of alloplastic materials achieved and maintained in bone during functional loading'.[11] Recently, Albrektsson *et al.* suggested that commercially pure Ti might act as a foreign body when placed in living tissues; hence hard tissue integration can be considered as an immune-modulated inflammatory process.[12] Conversely, a previous *in vivo* study predicted the possibility of a non-physical, bio-affinitive bond between Ti and bone.[13] The nature of interaction between bone and biocompatible implant surfaces, including Ti and zirconium dioxide (zirconia, ZrO_2), remains incompletely understood.

When an implant is inserted into a hole in the bone during implant surgery, water and ions come into contact with the implant surface during bleeding. As bleeding and hemostasis proceed, extracellular matrix (ECM) proteins mediate cell attachment to cover the surface.[14] Inflammation occurs and subsides, and granulation tissue formation and angiogenesis follow.[15] Osteoprogenitor cells adhere to the implant surface *via* the ECM proteins and differentiate into osteoblasts, which form new bone at the bone–implant interface.[14] Initially, the new bone is woven bone, which is replaced by lamellar bone, depending on load distribution and the resulting bone strain at the bone–implant interface.[15,16] Osteoclasts absorb the woven bone, forming resorbed depressions called Howship's lacunae. Osteoblast precursor cells detect the texture of this resorbed bone surface using pseudopodia, acquiring information on the quantity of bone needed to fill the lacunae.[17] Topographical modification of the implant surface to generate a texture similar to the lacunae is believed to enhance osteoblast bone formation activity.[18,19]

Dental implants made of Ti, particularly those made with commercially pure Ti, are widely used to replace lost teeth. Long-term successful clinical results (*i.e.*, >10 years) have been achieved with Ti dental implants.[6] Ti is a biologically stable metal that is inert and consistent, and does not activate biocompatible responses or foreign-body reactions when inserted in the human body.[20,21] Hard tissue integration allows implants to act as load-bearing structures. As implants are in direct contact with the surrounding bone, the stress applied on artificial crowns is transferred and distributed from abutments and implants to the underlying bone. A macroscopic design should be incorporated into implants to facilitate effective transfer of force to the bone and effective conversion of shear force to compressive force.[5] A representative example of such macroscopic design is a thread, and screw-shaped implants have been very successful clinically.[5,6]

Nevertheless, microscopic modifications of implant surfaces are necessary to accelerate hard tissue integration and reduce the duration of edentulous periods for patients, since most are aged, with consequent slow bone metabolism.[7,14] Bone response at the bone–implant interface plays a significant role in successful osseointegration, as demonstrated by *in vivo* studies showing that microchanges or nanochanges on the surfaces of Ti dental implants influence bone reactions.[7,22–25] Several studies have reported the effects of altering implant surfaces on accelerating and strengthening bone healing, allowing more rapid delivery of an implant-supported prosthesis to the patient.[25] Various types of surface treatment improve surface biocompatibility and bone regeneration around the dental implant, resulting in rapid hard tissue integration.[22,24,26–31]

Surface modification is achieved at the microscale or nanoscale. At the microscale, the surface of the implant is mainly modified topographically, usually to mimic the lacunae.[19] The roughness and morphology of this micro-topographically altered surface can be revealed by scanning electron microscopy (SEM).[14] At the nanoscale, treatment involves biochemical alteration of the implant surface (*e.g.*, application of molecules with affinity for osteogenic cells).[7,25] Surface control at the nanoscale is usually undetectable by SEM, because nanomodification has little effect on surface micromorphology;[25,32] however, for unknown reasons, osteogenic cells behave quite differently on nanomodified surfaces than on surfaces without nanomodification.[32]

Two important micro-topographically altered surfaces are established for use in the clinic: the sandblasted, large-grit, acid-etched (SLA) surface and the oxidized Ti surface. Implant surfaces can also be modified chemically by adding calcium (Ca) and phosphorus (P), the major elements of bone, or with trace amounts of fluoride, and these types of nano-modified surfaces have been successfully implemented in the clinic.

2.2. Modifications of surface topography

2.2.1. Surface modifications at the microscale. The three-dimensional structure of the implant surface consists of many elements and characteristics: form, configuration, shape, macrostructure and microirregularities.[33] Surface topography is usually defined by three characteristics: (i) lay, (ii) waviness, and (iii) surface roughness.[14] 'Lay' is the direction of the major surface pattern, usually determined by the manufacturing process. 'Waviness' is a measurement of the more widely spaced parameter of surface topography. 'Surface roughness',

specifically the arithmetic mean height of the surface (S_a), is used to classify Ti dental implant surfaces. Macroroughness in implantology has S_a values larger than 10 μm, which includes implant thread geometry.[33] The surface roughness whose S_a ranges from 1 μm to 10 μm is usually classified as microroughness.[7,33] Nanoroughness has dimensions ranging between 1 nm and 100 nm.[7,25,33] In this section, we focus on microroughness, in which S_a ranges from approximately 1 to 5 μm; we also discuss macroroughness (including Ti dental implant geometry and threads) and nanoroughness (S_a < 100 nm). The classification of microroughness is based on Albrektsson and Wennerberg's system, in which smooth surfaces have S_a < 0.5 μm; minimally rough surfaces have S_a = 0.5–1.0 μm; moderately rough surfaces have S_a = 1.0–2.0 μm (considered optimal for bone responses); and rough surfaces have S_a > 2.0 μm.[20]

The turned surface of a Ti dental implant does not undergo a modification process. Computer numerical controlled milling for surface machining yields various characteristics on this surface, such as machining grooves on a smooth surface (Fig. 3A). As mentioned above, a surface with S_a < 0.5 μm is classified as smooth. Although Ti dental implants with this type of surface yield successful long-term clinical results for restoration of missing teeth, a long period of time is required for osseointegration to occur prior to loading.[34] Consequently, turned surfaces are used as controls in many laboratory and clinical investigations to assess the qualities of modified surfaces.[14,24,30]

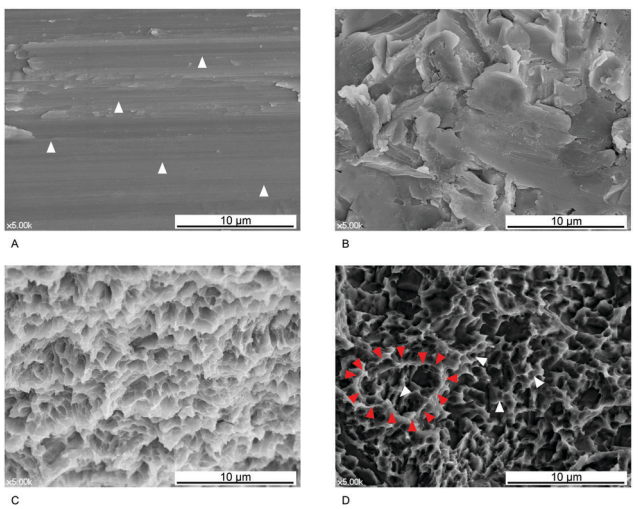

Fig. 3 (A) Scanning electron microscopy (SEM) image of turned Ti. The process of machining *via* computer numerical control milling yields characteristic grooves (white arrowheads). (B) SEM image of a blasted Ti surface. Many irregularities are formed during the blasting procedure. The surface morphology is affected by the diameter of the blast media (here, approximately 50 μm), the type of media (here, Al_2O_3), and the blasting pressure. In general, the irregularities are larger than those formed during etching. (C) SEM image of a Ti surface modified by acid etching showing small honeycomb-shaped irregularities resulting from the etching process. (D) Ti surface sandblasted with large particles (here, approximately 75 μm), followed by acid etching (Deep Implant System, Inc., Seongnam, Korea) imaged by SEM. The irregularities include large crater-like structures created during the blasting process (red arrowheads) and small honeycomb-shaped micropits (white arrowheads) produced by application of acids to the surface.

The surface of implants can be topographically modified by physical blasting (or grit blasting) with specific particles, called blast media. The most commonly used blast media in dental implantology are aluminum oxide (Al_2O_3), Ti dioxide (TiO_2), and CaP particles (Fig. 3B).[25] Various factors influence the resultant roughness, including the size of the particles, the duration of blasting, pressure, and the distance from the particle nozzle to the surface.[14,25] The optimal blasted surface with the best removal torque and bone-to-implant contact (BIC) is classified as moderately rough, with an S_a of approximately 1.5 μm.[35] Surface etching of Ti dental implants is commonly achieved using hydrochloric acid, sulfuric acid, and hydrofluoric acid (HF).[25] Commercially pure Ti contains trace impurities that are acid-labile, while elemental Ti is resistant to corrosion by acid; therefore, when a Ti implant is immersed in an acidic solution, the acid can cause erosion and formation of surface pits. Acidic solution type, concentration, temperature, and etching period can all influence the microstructure of the etched surface.[14] The diameter of the pits produced in this manner is typically 0.5–2 μm (Fig. 3C), and the S_a value of the etched surface is <1.0 μm.[14] Consequently, the surface may be smooth or minimally rough.

The surface of a Ti dental implant can be sandblasted with large grit particles (75–500 μm in size) and then immersed in an acidic solution for etching, yielding an SLA surface (Fig. 3D).[7,19,25] SLA surfaces have been widely used in clinical dentistry for many years; however, the resultant surfaces differ topographically depending on the conditions used for etching and blasting.[19,22,24] Bone formation activity of osteogenic cells on an SLA surface is believed to depend on the microtopographical similarity of the surface to the lacuna, the site where osteoclasts resorb the bone.[19] Most previous studies have described SLA surfaces as moderately rough, and more biocompatible than surfaces that are only etched or blasted.[36,37] Therefore, SLA surfaces serve as positive controls in studies evaluating new modified surfaces.[38–41]

Another type of SLA surface used in clinical dentistry has additional hydrophilic properties, and is called a hydrophilic SLA or modified SLA (modSLA) surface. An SLA surface with no additional hydrophilicity is considered a standard or hydrophobic SLA surface. To make a standard SLA surface hydrophilic, it is rinsed in water under nitrogen protection and stored in isotonic NaCl solution without atmospheric contact.[42] Implants with hydrophilic SLA surfaces are similar to those with standard SLA in terms of topography (Fig. 4A) (*i.e.*, they have moderate roughness); however, a few studies have reported modSLA surfaces with S_a > 2.0 μm, which were therefore classified as rough.[23,43]

When exposed to oxygen in air, the implant surface naturally develops a Ti-oxide layer that can be thickened by making the surface an anode in a galvanic cell and applying voltage to the electrolyte solution.[44–46] Following such treatment, multiple micropores of various sizes are observed on the oxidized surface in SEM images (Fig. 4B). Using this approach, the surface roughness (often minimally rough) and surface characteristics of

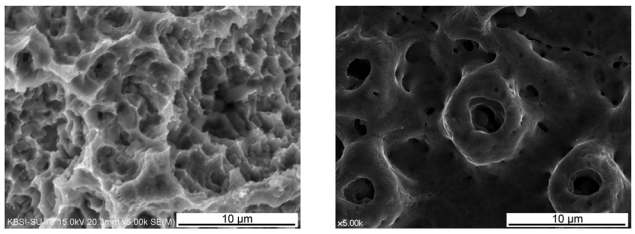

Fig. 4 (A) Scanning electron microscopy (SEM) image of a hydrophilic SLA surface (SLActive, Institute Straumann AG, Basel, Switzerland). There are no distinct differences in specific SEM features between hydrophilic and standard SLA surfaces. (B) SEM images of an anodically oxidized Ti surface (TiUnite, Nobel Biocare, Zürich, Switzerland) displaying protruded open pore micro-structures.

Ti dental implants can be changed by varying the applied voltage, the electrolyte content, and the duration of oxidation.[14] In addition, the Ti oxide layer (but not Ti itself) is biocompatible.[7] Therefore, layer thickening and roughening of the topography of Ti oxide by anodic oxidation are considered to increase the biocompatibility of the implant surface.

Diverse biocompatible surfaces have been developed and tested for potential future clinical use. In general, evaluation of bone responses to modified surfaces follows a hierarchical approach, as follows:[47]

(1) Surfaces are tested *in vitro*, and various properties (*e.g.*, cell adhesion, spreading, and expression of important marker genes) are evaluated.

(2) *In vivo* animal research, including histomorphometric evaluation, is performed.

(3) Retrospective and/or prospective clinical investigations follow.

Many laboratory and clinical studies have evaluated modified implant surfaces using a turned (*i.e.*, unmodified) surface as a control.[7,48] Standard SLA, modSLA, and oxidized surfaces have yielded improved results both *in vitro* and *in vivo*, relative to turned surfaces.[49] Such topographically modified Ti dental implants achieve high survival rates in clinical trials,[34,50–53] and there is some evidence that modSLA surfaces result in faster bone healing and stronger osteogenic effects than their predecessor standard SLA surfaces;[54,55] however, many studies failed to detect significant differences in bone responses among modified surfaces.[49,56,57] Some studies found no significant differences between standard SLA and oxidized surfaces *in vitro* or *in vivo*, while there are other studies that reported that modSLA surfaces yield improved results compared with standard SLA or oxidized surfaces.[24,54,58] Topographical features other than roughness may affect bone responses to the implant surface; however, it remains unclear how these features affect bone responses. It is unknown whether the honeycomb morphology of SLA surfaces (Fig. 3D) or the volcano-like micropore morphology of oxidized surfaces (Fig. 4B) are more compatible with bone healing, although implant surfaces similar to the microtopography of the osteoclast resorption site are believed to stimulate bone formation activity in the biological environment.[19]

Micro-topographical changes on the implant surface induce accelerated bone healing and stronger osseointegration around the implant relative to turned-surface implants. At the cellular level, modified surfaces with higher S_a than turned surfaces stimulate osteogenic cell attachment, spreading, and activation.[25,59] At the tissue level, dental implants with topographically modified surfaces exhibit faster bone healing.[7,60,61] Clinically, topographically modified implants are believed to be more suitable for early loading than turned implants, although both types of implants have proved successful in clinical trials following conventional loading protocols.[48,62–64] Importantly, however, the exact roles of altered roughness and other topographical features (including chemical features) resulting from surface treatments remain poorly understood.

2.2.2. Nanoscale surface modifications. Anodic oxidation of the Ti surface in an appropriate solution containing hydrofluoric acid produces TiO_2 nanotube arrays with a diameter ranging from 10 to 100 nm by adjusting the electric current of the electrochemical cell, temperature, the pH values of electrolyte solutions, the electrolytes, oxidation voltage and oxidation time.[25,65–68] These nanotopographical features improve protein adsorption and osteogenic cellular responses.[67–69] The hard tissue responds favorably to this TiO_2 nanotube-arrayed surface.[70,71]

The optimal diameter for osteogenic reaction has been reported to be within 100 nm although similarity to pores found in bone tissue is closer to microirregularity induced by SLA treatment.[19,25,66,72,73] In a previous study, TiO_2 nanotube arrays whose diameter was 15 nm showed most active cell behaviors in adhesion, proliferation, migration and differentiation.[66] Another previous study reported that the layer of TiO_2 nanotubes ranging from 70 nm to 100 nm was more effective in osteogenic cell differentiation of mesenchymal stem cells and that of 30 nm nanotubes was more advantageous in cell adhesion and proliferation.[74] However, there was a prior investigation confirming that TiO_2 nanotubular structures with a diameter of 80 nm promoted both proliferation and differentiation of mesenchymal stem cells more than those with a diameter of 20 and 40 nm.[75] Crystallinity of nanotubes (anatase, rutile or amorphous) is related to surface wettability, which affects adhesive protein adsorption and osteogenic cell response in bone healing.[25,76,77] However, the exact mechanism of the effect of crystallinity on bone healing is unclear. Several *in vivo* studies reported excellent osseointegration on modified TiO_2 nanotubular surfaces.[78–80]

The TiO_2 nanotubular structure is able to load biofunctionalizing molecules to enhance the hard tissue integration and to deliver drugs for local therapeutic effects.[81–85] In fact, this implant surface modification has been evaluated for osteogenic potential with a combination of bioactive molecules including growth factors.[82,86,87] The feature of drug release from TiO_2 nanotubes has been utilised for local therapies, which mainly produce osteogenic effects in compromised bone conditions such as osteoporosis and antibacterial effects.[79,81,88–90] The drug release has been found to be effective when the diameter of TiO_2 nanotubes is larger than approximately 100 nm, which is slightly different from the optimal diameter for osteogenesis.[90,91]

TiO_2 nanotubular topography has antibacterial properties with carriage of antibiotic drugs or metal doping.[89,92–94] The TiO_2 nanotube layer is capable of antibacterial effects by tuning the tubular geometry and physico-chemical properties.[95] For example, the wettability of TiO_2 nanotubes was reported to hinder bacterial adhesion.[69] However, further investigation is necessary to understand the antibacterial mechanism of the hydrophilicity of TiO_2 nanotubes. Some previous studies reported that the hydrophilic properties of the TiO_2 nanotube layer reduced bacterial adhesion, whereas other investigations interpreted that the decrease in bacterial adhesion is due to hydrophobic properties.[92,96,97]

TiO_2 nanotube arrays have broad applicability. However, this modified surface at nanoscale has not been used in dental clinics yet. No published clinical trial has been found and other nanoscale forms including nanorods and nanopores have also not been in clinical use. The wear resistance to delamination of the TiO_2 nanotube arrays is a concern despite a high wear resistance to friction occurring during implant insertion into the bone.[25,65] Other concerns are the side effects of doped or loaded materials. Particularly, some metal ions including silver, copper and even gold are cytotoxic in a certain biological condition although these ions incorporated on TiO_2 nanotubes are well known for antibacterial functions.[89]

2.3. Modifications with surface compounds

2.3.1. Application of non-organic compounds to dental implant surfaces. Coating Ti surfaces with CaP compounds is thought to make the surface bioactive.[20] Such surfaces are highly osteoconductive (bridging between the existing and the new bone) to the surrounding bone, and can be osteoinductive (inducing the osteogenic process) when used with bone morphogenetic proteins (BMPs).[20,98] Ca and P are the main elemental components of human bone, and are considered to endow Ti with biocompatibility; therefore, CaP coating of implant surfaces is conducted by various methods including plasma spraying, which is a major CaP coating technique.[99,100] Briefly, hydroxyapatite (HA) particles are injected into a plasma flame at high temperature (approximately 15 000–20 000 K), and the heated particles are then projected onto the Ti implant surface, forming a CaP coating of around 50–100 μm thick on the surface.[36] Bone responses to CaP coating are influenced by its uniformity, crystallinity, and composition (Ca/P atomic ratio).[99] Manipulation of the Ca/P ratio can accelerate or decelerate dissolution and degradation of the coating layer in the biological environment.[99]

Clinically, CaP-coated Ti dental implants have proven successful and functional over long service periods.[101,102] The *in vivo* biomechanical removal torque and histomorphometric BIC of CaP-coated Ti dental implants are reportedly higher than those of turned or blasted implants, indicating earlier and faster bone healing and osseointegration.[103] Nevertheless, plasma spraying has many limitations, including possible coating layer delamination and cohesive failure.[99] Further, CaP coating by plasma spraying obstructs bone apposition at the dissolving area and attracts inflammatory cells.[104] Consequently, dental practitioners have a negative view of CaP-coated implants. Considerable efforts have been made to develop new methods to replace plasma spraying for CaP coating.[105]

When using Ti dental implants in patients with limited bone quantity or quality, various features of CaP coating make it particularly attractive, including its excellent osteoconductivity and osseointegration with the surrounding hard tissue.[99] Thin CaP coatings have been developed using various methods, including sol–gel deposition and ion sputtering (Fig. 5).[24,105,106] These approaches change the nanoscale surface topography of the implant and decrease the thickness of the CaP film coating.[107–109] Typically, CaP coating thickness ranges from 1 to 5 μm, and the size of the coated materials ranges from 20 to 100 nm.[107,108]

CaP-Coated Ti dental implant surfaces modified at the nanoscale exhibit superior osseointegration and higher bioactivity than uncoated Ti dental implant surfaces.[110,111] Ion beam-assisted deposition is another method used to coat implant surfaces with CaP.[110,112] The thickness of the coating formed using this approach is around 500 nm.[110] Briefly, disc-form evaporants (HA + 37% calcium oxide [CaO]) are sintered inside a vacuum chamber for 2 h at 1000 °C.[110] An electron beam is applied to the vacuum chamber, and HA and CaO evaporate and adhere to the implant surface.[110,113] When CaP is nanocoated onto implants with different textures in various bony environments, no difference in osseointegration is observed between roughened and smooth surfaces with sufficient bone area, whereas CaP nanocoated onto a roughened Ti dental implant surface increases osseointegration in a bone-deficient environment.[110] Ti dental implants with CaP nanocoating on a minimally rough etched surface are commercially available (Nanotite, Biomet 3i, Palm Beach Gardens, FL, USA).

Fluoride (F^-) is specifically attractive to Ca and P, the major elements of human bone.[114] The surface of grade 4 commercially pure Ti is reduced at the cathode when it is immersed in a dilute solution of HF, which attracts fluoride ions to the implant, and the resultant surface is fluoride-modified.[7,115] In the dental implant market, only OsseoSpeed (Astra Tech, Dentsply, Waltham, MA, USA) uses a fluoride-modified surface. To generate these implants, a low concentration of hydrogen fluoride is applied to a Ti surface blasted with TiO_2 particles. This cathodic reduction results in fluoride incorporation into TiO_2 without a significant change in surface microstructure.

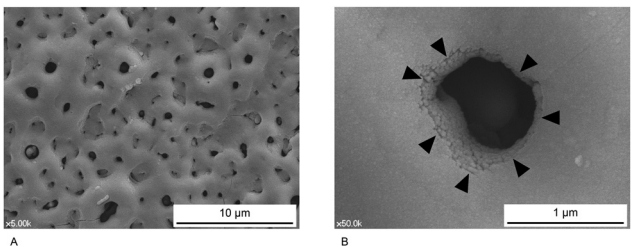

Fig. 5 Ion beam deposition is used to apply CaP on the anodized Ti surface (Dentium, Seoul, Korea). (A) In low-magnification SEM images, it is difficult to detect nanotopographical changes caused by CaP. (B) The CaP layer (black arrowheads) can be seen in higher magnification SEM images.

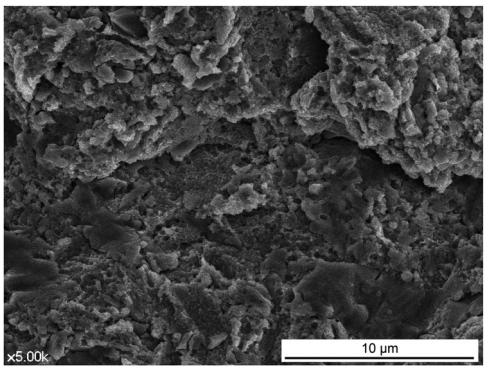

Fig. 6 Image of a fluoride-treated surface (Osseospeed, Astra Tech, Dentsply, Waltham, MA, USA). After blasting with Ti dioxide particles, the surface is treated with fluoride. Consequently, the surface is similar to those blasted with Ti dioxide particles alone.

In terms of roughness, the S_a of the OsseoSpeed surface is approximately 1.5 µm, making it moderately rough (Fig. 6).[117,118] X-ray photoelectron spectroscopy can detect trace amounts of fluoride on the implant surface, but energy-dispersive spectroscopy detects no fluoride content.[23,26]

Fluoride acts primarily on osteoprogenitor cells and undifferentiated osteoblasts, but not on differentiated osteoblasts, by increasing growth factor synthesis, facilitating their differentiation into osteoblasts.[119] Further, the nucleation capacity of Ca and P ions improves on a fluoride-modified Ti dental implant surface.[116] Thus, fluoride may accelerate early bone responses to a modified Ti surface, thereby promoting bone healing. Several *in vitro* cell studies have demonstrated enhanced expression levels of various osteogenic marker genes on fluoride-modified Ti implant surfaces.[116] Moreover, *in vivo* animal experiments revealed faster bone healing and mineralization on a fluoride-modified implant surface than on a TiO_2-blasted surface without fluoride modification.[116,120] Clinically, fluoride-modified Ti dental implants are successful in early loading, with 5 or even 10 year survival rates greater than 95%.[121–123]

Fluoride-modified Ti dental implant surfaces are considered bioactive because, like CaP-coated surfaces, they interact with bone at the BIC more strongly than topographically modified surfaces.[20] Fluoride-modified Ti dental implant surfaces likely benefit from the combined effects of modified topography and chemistry. Specifically, such surfaces bind strongly to bone; cutting the interface between the bone and the modified surface is significantly harder than cutting between the bone and the original surface without fluoride treatment.[115] Interestingly, the higher quality of newly developed Ti dental implant surfaces is not observed, when compared to other micro-roughened implant surfaces. *In vivo* studies detected no significant difference in histomorphometry when fluoride-modified surfaces were compared with oxidized or SLA surfaces.[26,124] Likewise, one *in vivo* study reported similar early bone responses between CaP-coated and blasted surfaces.[125] Further investigations are needed to explore the effects of these bioactive inorganic elements on bone responses.

Dental implant surface topographies modified at the nanoscale are expected to contribute to accelerating bone responses; however, in contrast with microscale modifications, the benefits and effects of nanomodifications are not yet fully understood at the cellular or tissue levels. In addition, the optimal size and distribution of nanoparticles for application to dental implant surfaces remain unclear. The limitations of the micro- and nano-controls of the surface should also be considered. Even bioactive coatings, such as CaP, have failed disastrously in clinical settings when coated onto the surface of cylindrical Ti dental implants.[126,127] After threads were added to dental implants (*i.e.*, conversion of cylinders into screws in terms of macroscale geometry), the same bioactive coating became successful in long-term clinical use.[128–130]

2.3.2 Application of organic compounds to dental implant surfaces. When a dental implant is inserted into the bone, ECM proteins adsorb to the implant surface during hemostasis.[15] Several ECM proteins are involved in the adhesion of osteogenic cells.[14] Osteoblasts express transmembrane proteins that recognize adhesion molecules, including laminin and vitronectin.[15,30,131] One family of transmembrane proteins, the integrins, has been extensively studied. Binding of integrins to ECM proteins is an important process through which osteoblasts interact with the ECM, and this relationship controls cell morphology, proliferation, and differentiation.[132] Integrins mediate cell adhesion, subsequent cell signaling, and interactions related to bone healing.[132,133] Adhesion proteins coated on the implant surface can accelerate the bone response, because bone healing begins with the attachment of osteogenic cells to the surface.[14] Small active amino acid sequences (functional peptides), derived from the original adhesion proteins, can be more attractive as coating materials than the whole proteins, which are large (causing undesirable immune reactions in the host) and multifunctional (making cellular reactions difficult to control).[30,59] Adhesion molecules on dental implant surfaces bind to osteoblast receptors (transmembrane proteins) and trigger intracellular events, leading to cellular activation.[30,39,59,131]

Functionalized dental implant surfaces coated with arginylglycylaspartic acid (RGD) peptides exhibit superior histomorphometric results, indicating accelerated osteogenesis relative to uncoated surfaces.[134] Recently, two functional peptides involved in cell adhesion have been identified in human laminin:[30,59] DLTIDDSYWYRI (12 amino acids) and PPFEGCIWN (nine amino acids). These two peptides also actively bind to osteogenic cells, and a mechanism by which they can trigger intracellular cascades has been proposed (Fig. 7).[30] Such laminin-derived functional peptides appear to overwhelm the topography and chemistry of the underlying dental implant surface during bone cell attachment, although both the implant surface structure and coating organic compounds affect cellular and tissue responses.[59] A functional peptide derived from another adhesion protein, vitronectin, also has strong potential to accelerate bone healing at the bone–implant interface.[38,131]

Other biomolecules that can enhance bone healing include cytokines, particularly growth factors.[7,25] Further, BMPs are candidates for use in clinical dental implantology. BMPs are temporal signaling molecules with complex biological effects

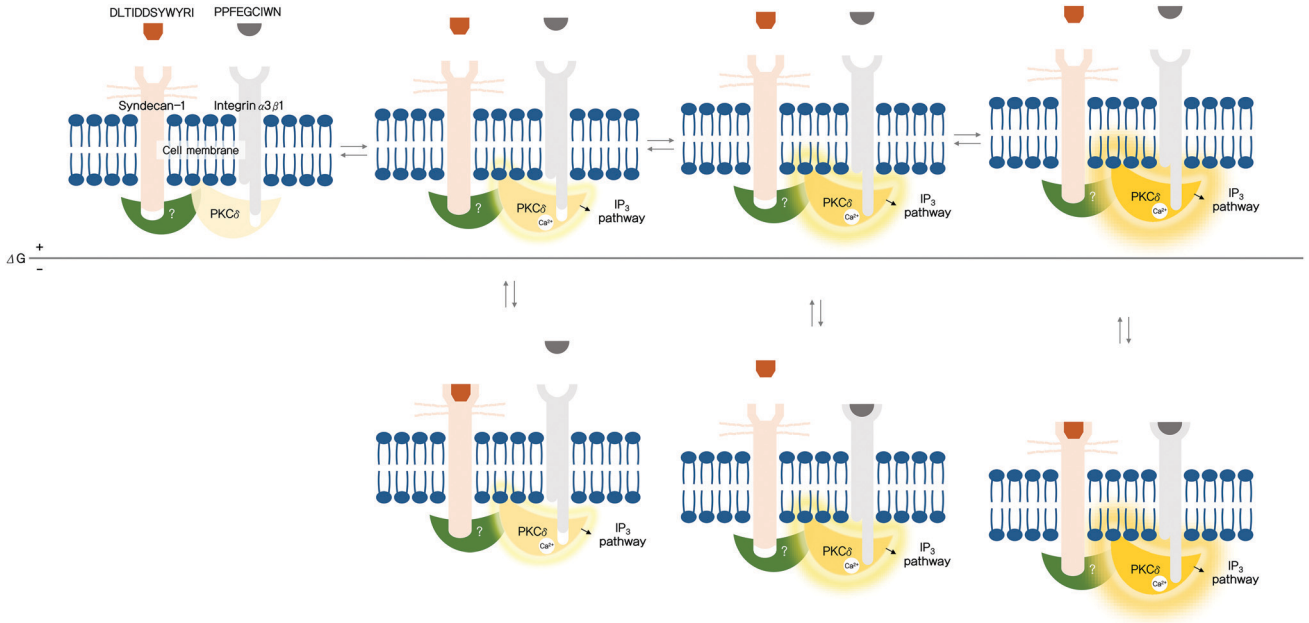

Fig. 7 Proposed mechanism, based on a probabilistic interpretation of allostery for two laminin-derived bioactive peptides.[14,30] (Reproduced from ref. 14 and 30 with permission from Elsevier.) The black horizontal line indicates that the Gibbs free conformational energy difference (ΔG) is zero. A more stable energy state is shown below the line. The degree of enzyme activation is demonstrated through the brightness and intensity (red lines) of protein kinase Cδ (PKCδ). When functional peptides bind to transmembrane proteins with tunable sensitivity for PKCδ phosphorylation, various conformational energy states are adopted. Even if the peptides do not bind to their receptors, PKCδ can be reversibly activated. Thus, when neither of the peptides binds to the transmembrane receptors, an equilibrium is reached between the inactive (far left) and active states; however, such activated states are likely short-lived due to their high free energy. Circumstances differ when either PPFEGCIWN or DLTIDDSYWYRI, or both peptides bind to the receptors. Binding significantly stabilizes the conformations, increasing the probability of the active states. An increase in the number of active states effectively triggers intracellular events *via* the transmembrane proteins, promoting cell adhesion. Glow of PKCδ represents the extent of activation (more active to the right). IP_3, inositol triphosphate; Ca^{2+}, calcium ions; (?), unknown protein.

that depend on their concentrations and the conditions of surrounding tissues. Human recombinant BMP-2 (rhBMP-2) is currently used in the clinic, and rhBMP-2-coated Ti dental implants accelerate bone healing *in vivo*;[135,136] however, cytokines are not adhesion molecules, and BMPs are ineffective when coated onto surfaces because their bone-healing effect requires free diffusion in the tissue microenvironment.[116] A previous study reported that BMP-2 applied directly to osteoblastic cells promotes cellular adhesion to Ti dental implant surfaces by increasing adhesion molecule expression.[137] Some studies have reported conflicting results concerning BMP-2, including osteolysis or negative effects on osteogenesis around BMP-2-treated implants.[138–140] Moreover, it is difficult to directly coat BMP-2 on to Ti. Some studies used BMP-2 in free form, whereas others coated BMP-2 on a surface modified by application of CaP, other growth factors or the anodic oxidation technique, and the effects on bone responses were mixed.[110,135,136,141,142]

To establish a more biomimetic environment at the bone-healing site, a growth factor can be combined with dental implant surfaces coated with an adhesion molecule. One study proposed that adhesion molecules can exert bone-induction effects in the presence of BMPs.[143] Dental implant surfaces functionalized with adhesion molecules and nanocarriers are also applicable; in this setup, nanocarriers contain growth factors and release them in free form after implant insertion. The initial bone response and subsequent bone remodeling can be manipulated by controlling the time of release of the contained factors. The peptide-functionalized implant surface is predicted to control the biological environment, which leads to implants that are more readily available for edentulous patients with some metabolic disorders; for example, a Ti implant treated with a vitronectin-derived peptide stimulates osteoblast activity and inhibits osteoclast activity, making it a candidate device for osteoporotic patients.[131]

This section has focused mainly on modified implant surfaces successfully used in clinics; however, implants more readily applied in patients with certain metabolic diseases and peptide-treated implant surfaces warrant consideration for future use, although these surfaces have yet to be employed in the clinic.

Immobilizing peptide molecules on an implant surface is another major challenge. Physical adsorption is the simplest and easiest method for immobilization, where peptides are non-covalently applied on the surface;[144] this is the main methodology employed in many previous studies and is effective for maintaining molecular activity, due to low dependence on peptide conformations, which are critical in determining the activities of the original proteins;[30,38–40,131,144,145] however, this immobilization strategy poses difficulty in delivering sufficient peptide molecules to target sites.[144] Conversely, covalent immobilization methods are resistant to the damage associated with

peptide layers applied during dental implant installation, whereas process complexity related to covalent bonding, purification, detoxification and monitoring, and additional costs are obstacles to the transition from laboratory to manufacturing scales.[144] If peptide-functionalized implants are clearly shown to display stronger osseointegration in edentulous patients with bone metabolic disease, new or established immobilization techniques may be applied to manufacture dental implants.

3. The gingiva–abutment interface (soft tissue seal)

3.1. The soft tissue seal

The tooth penetrates the gingiva to connect external and internal environments. The root of the tooth is fixed in alveolar bone, and the transition region contacts epithelial and connective mucosal tissue. The hole (or flaw) formed by a tooth is sealed by a special structure consisting of epithelial tissue and connective attachment in the transition region. The epithelial tissue is attached to teeth by the internal basal lamina and hemidesmosome, and the connective tissue adheres through a combination of dento-gingival fibers and cementum.[146] Thus, the soft tissue attachment seals the flaw, and the tooth generates the hole connecting the external and internal environments. In a dental implant, the soft tissue attachment is similar, but not identical to that of natural teeth (Fig. 8A).[147]

A dental implant is anchored to alveolar bone and the abutment contacts the soft tissue (epithelial and connective tissue) in the transition region. The connective tissue attachment to the abutment of a dental implant does not involve dento-gingival fibers, which adhere perpendicularly to cementum in natural teeth. The collagen fibers around the abutment mainly run parallel and circularly to the surface. The connective tissue attachment around the abutment is maintained by the elasticity of circular fibers and fibroblasts holding the collagen fibers, unlike the natural teeth, where the fibers are directly inserted (Fig. 8A).[148] Therefore, the connective tissue attachment around the abutment must be weaker than its counterpart in natural teeth. The epithelial attachment around the abutment is also weaker than that in natural teeth, due to the restricted

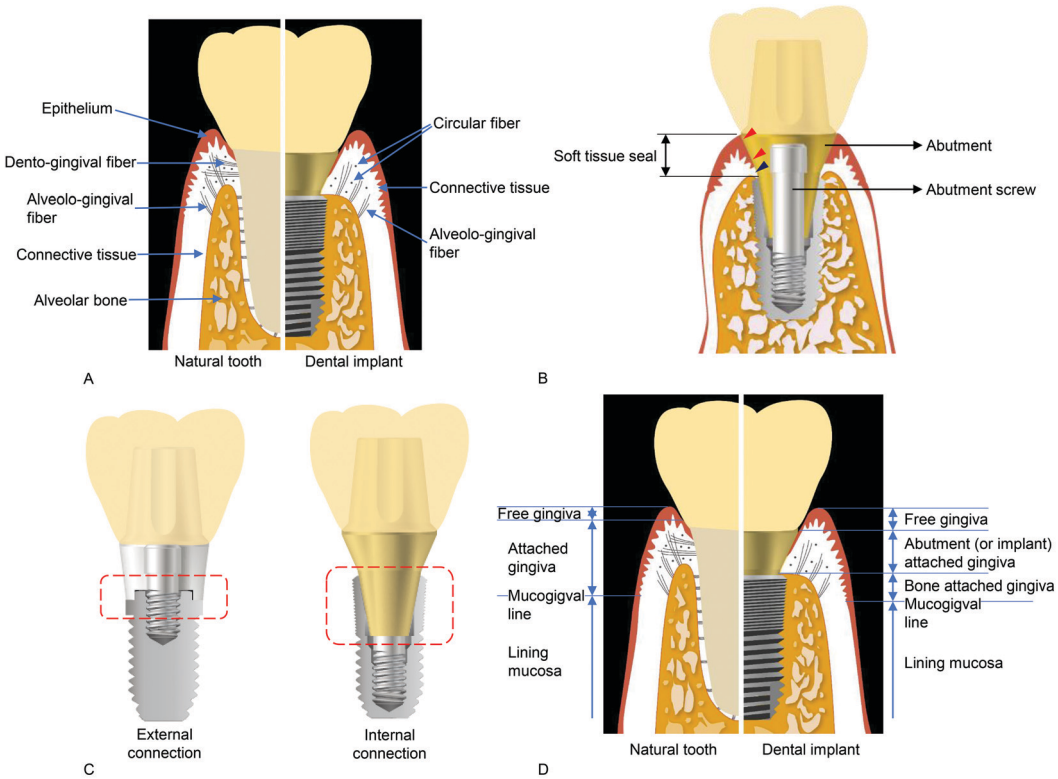

Fig. 8 (A) Soft tissue and collagen fibers around a natural tooth (left) and a dental implant (right).[5] (Reproduced from ref. 5 with permission from Multidisciplinary Digital Publishing Institute.) Note that there are no dento-gingival fibers surrounding the implant. (B) Soft tissue seal and abutment screw (cross-section of an implant-supported restoration). An abutment screw clamps the abutment and implant, and the stability of the connection determines the stability of the soft tissue seal, consisting of epithelial (red arrowheads) and connective tissue (blue arrowhead) attachments. (C) A typical example of an external connection (left) and an internal connection (right). Dashed red boxes show the difference in mating surfaces between the two connections: a butt-joint, or an abutment placed on the implant platform, is shown in the external connection, while friction occurs between the inclined planes of the implant and abutment, contributing to abutment stability. (D) Schematic diagram of the soft tissue structures around a natural tooth (left) and a dental implant (right). Note the gingiva directly attached to the surfaces of implant parts, indicating that the sealing capability of this structure is lower than that surrounding the natural tooth.[5] (Reproduced from ref. 5 with permission from Multidisciplinary Digital Publishing Institute.)

distribution area of the internal basal lamina and hemidesmosomes.[149–155] Thus, the soft tissue attachment (epithelial and connective tissue attachment) sealing the hole (or flaw) is weaker around implants than that in natural teeth.

The soft tissue seal, or mucosal seal, is another important factor determining long-term implant success.[5,156,157] The soft tissue seal around a dental implant is defined as the attachment of epithelial and connective tissues to the surfaces of the implant system, mainly the abutment surface.[5] It is necessary to understand both the abutment surface directly attached to soft tissue and the mechanics of abutment-to-implant connection *via* an abutment screw, because the unstable state of the connection from the mobile abutment leads to breakage of the soft tissue seal (Fig. 8B and C).[48,158]

In dental implantology, an implant and an abutment are connected through a unique mating structure. When an abutment connects to the 'outer' structure of an implant, it is referred to as the 'external' connection, while abutments connected to the 'inner' structure of an implant are called 'internal' connections (Fig. 8C). Originally, implant–abutment connection stability was accomplished using an abutment screw alone;[6] however, due to mechanical complications associated with the screw, a more stable connection has been achieved using a specific mating structure between the implant and the abutment, to minimize the role of the abutment screw.[5,159] The most important feature, for both external and internal forms, is whether movement is allowed between an abutment and the connection structure. Most biological and mechanical complications of dental implant systems are related to the mobility of implant-to-abutment connection.[160]

3.2. Importance of the soft tissue seal

The complete immobility of the soft tissue contact to the abutment is important for the long-term predictability of implants.[5] If peri-implant soft tissue is mobile, the attachment will be severed because the structure is weaker than that in natural teeth, resulting in disruption of the soft tissue seal.[5,148,156] Bacteria can invade through the damaged mucosal seal, resulting in peri-implant disease or inflammation.[156,157] Therefore, the soft tissue seal is the most important factor in preventing peri-implant disease because it protects against bacterial invasion.[157,161]

The mucosa around natural teeth is classified as either masticatory or lining mucosa, where masticatory mucosa consists of free gingiva and attached gingiva (Fig. 8D). Attached gingiva is responsible for soft tissue immobility by tightly attaching to the surface of enamel, cementum, and alveolar bone.[146] Thus, immobility contributes to preserving a firm and healthy soft tissue seal. The components of soft tissue around implants are essentially similar to those surrounding natural teeth; however, the attached gingiva around implants differs.[147] Attached gingiva around implants is either bone-attached or abutment (implant)-attached (Fig. 8D). Bone-attached gingiva is the same as that of natural teeth, and provides solid immobility, whereas abutment-attached gingiva is weaker, and approximately equal in strength to free gingiva.[147] Therefore, if bone-attached gingiva is of insufficient width to prevent mucosal mobility, peri-implant disease becomes more likely, due to the fragile structure of abutment-attached gingiva.[147,162]

3.2.1. Disruption of the soft tissue seal. There are two reasons why the soft tissue seal may become disrupted: mobile soft tissue and unstable implant–abutment assembly.[5] First, a lack of bone-attached gingiva around an implant can result in rupture of the mucosal seal, due to soft tissue mobility, allowing bacteria to invade the internal environment and potentially leading to peri-implant disease.[162] Therefore, the presence of bone-attached gingiva is more important in implants than in natural teeth, due to the fragile soft tissue attachment around implants.[148,150] Positioning the implant in the center of attached gingiva during surgery contributes to preserving the bone-attached gingiva.

Second, unstable implant–abutment connection can also disrupt the soft tissue seal.[5,158] Dental implant systems comprise three parts: a prosthetic (artificial crown), a transition (abutment), and an implant. Transition part mobility can cause destruction of the mucosal seal. A mobile implant can lead to failed osseointegration, while a mobile abutment implies the mobility of the transition part, regardless of successful osseointegration. Abutment mobility is mainly caused by loosening of the abutment screw that stabilizes the implant–abutment assembly.[163] Loosening is more frequent in external than internal type implants, due to elongation and unscrewing of the abutment screw following lateral occlusal force.[164,165] Due to friction between the inclined planes of an implant and abutment, lateral occlusal force is concentrated in this type of internal connection, not on the abutment screw but on the implant wall through the abutment–implant connection area.[159,166] Therefore, screw loosening is less frequent in such internal type connections.[167] A wider abutment can avoid stress concentration on specific sites, including the abutment screw, and contribute more to soft tissue seal stability than a narrow connection. The soft tissue around implants can be maintained by support from healthy sub-alveolar bone, which should be stimulated appropriately to preserve healthy dynamic conditions.[16] The appropriate stimulation and distribution of strain can be achieved in wide and deep connections between these two parts (abutment and implant).[166]

3.2.2. Peri-implant disease. Transition into peri-implant disease occurs when the mobile soft tissue or the unstable implant–abutment connection causes mucosal seal disruption. Peri-implant disease can be classified into two categories, according to alveolar bone loss: peri-implant mucositis and peri-implantitis.[168]

(1) Healthy peri-implant shows neither bleeding on probing nor inflammation, with normal or reduced bone support. Peri-implant problems are not found in measured probing depth data.[169–171]

(2) In peri-implant mucositis, bleeding on probing and inflammation can be observed by visual inspection; peri-implant mucositis is mainly plaque-induced.[172]

(3) In peri-implantitis, bleeding on probing, inflammation around peri-implant mucosa, and progressive loss of supporting bone are observed. This is a plaque-associated pathological

condition of soft tissue around dental implants. Poor plaque control and a history of severe periodontitis both contribute to peri-implantitis.[173]

In practice, transition into peri-implant disease is caused by disruption of the mucosal seal, enabling bacterial invasion, but not by the bacterial plaque itself, although treatment of peri-mucositis and peri-implantitis can eliminate plaques.[168] Therefore, maintenance of a healthy mucosal seal, including by use of micro- and nanotechnologies to strengthen this soft tissue attachment, is much more significant than plaque control or antibacterial biomedical technology regimens. Immobile soft tissue and implant–abutment connection are important, since the mucosal seal around implants is weaker than that around natural teeth. Free gingiva and abutment (or implant)-attached gingiva are unable to provide immobility, unlike bone-attached gingiva and rigid connection between an implant and abutment.[174] Immobility contributes to maintain a healthy mucosal seal, protect against bacterial invasion, and thereby prevent transition into peri-implant disease.

3.3. Importance of abutments in the soft tissue seal

In general, an implant abutment is divided into three parts regardless of its mating type with reference to an implant; each part is determined by what is attached to it (Fig. 9A).

(1) The cementation part is a cylindrical structure connected to a prosthesis (artificial crown). This part is related to retention of the prosthesis, based on its resistance to disconnecting force. Retention is enhanced by increased height and narrower diameter.

(2) The transmucosal part is the surface where the soft tissue seal forms. This part is particularly important because oral bacterial penetration can occur where a dental implant pierces the oral mucosa. Therefore, the soft tissue seal in this region must be healthy and undisturbed to ensure implant longevity.

(3) The connection part is an interface where an abutment and an implant contact directly. This part is especially important in determining the longevity of an implant because it can transfer an occlusal load from a prosthesis to an osseointegrated bone.

As mentioned earlier, abutments and implants are strongly connected by abutment screws. Usually, a torque of 25 to 35 Ncm is applied to the screw for preload.[163] If the preload decreases for any reason, the connection between an abutment and an implant is loosened, the soft tissue seal is broken, and this can lead to peri-implant disease.[5,48,158,163] The use of an implant system with a mechanism by which stress is not concentrated on an abutment screw is therefore useful for the long-term clinical service of an implant.[48,158]

3.3.1. Butt joint *vs.* friction-fit joint. Before we compare butt joints and friction-fit joints, we need to describe the classification of joint types and explain the basic relationship between joint type and soft tissue seal. Occlusal force is applied to an abutment through an artificial crown, and then to an implant through the implant–abutment connection.[5,166] The implant–abutment connection must be sufficiently rigid to endure strong occlusal force.[175] The connection between an abutment and an implant can be simply classified as a butt joint or a friction-fit joint, based on the way these components are assembled (Fig. 9B). In terms of the role of the abutment screw, the butt joint is a 'screw-retained only connection (SR connection)', while the friction-fit joint is a 'friction and screw-retained connection (FSR connection)'.

In a butt joint, two right-angled flat surfaces mate, leaving a small space between the mating parts. By contrast, a friction-fit joint leaves no space between the mating parts, since the parts are forced together. The Brånemark implant, the first commercialized screw-shaped endosseous dental implant, has an external and hexagon-mediated butt joint connection, and similar types of implants have been manufactured and sold in the dental market worldwide.[176–178] The space in this joint type can cause movement of an abutment when occlusal load is applied. At one time, a microgap (a small gap formed between an abutment and an implant) was thought to cause marginal bone resorption by acting as a habitat for bacteria, thereby triggering marginal bone loss.[179–181] Based on this assumption, marginal bone resorption was considered an inevitable physiological phenomenon. More recently, Hermann *et al.* showed that marginal bone resorption resulted from abutment movement, not microgaps.[182] Thus, overall, evidence suggests that abutment movement can break the soft tissue seal around an abutment, potentially resulting in marginal bone resorption.[48,158] The friction-fit type can limit the movement of an abutment by friction generated at the interface, which may enhance the stability of the soft tissue seal, and prevent marginal bone resorption.[5,48,156,183,184]

3.3.2. Effects of abutment materials. Formation or lack of formation of a soft tissue seal may depend on the material attached to it.[161] One study evaluated the stability of the soft tissue seal using four materials: gold, dental porcelain, Ti, and aluminum oxide. No soft tissue seal could form using gold and dental porcelain, and marginal bone resorption occurred; however, with Ti and aluminum oxide, the soft tissue seal formed correctly, and no marginal bone was resorbed.[185] In 2008, Welander *et al.* similarly demonstrated diminished epithelial attachment when a gold alloy abutment was used.[186] Therefore, the use of an abutment designed at the University of California at Los Angeles, the so-called UCLA abutment, fabricated by gold casting, a popular prosthetic option at one time, can break the soft tissue seal and increase marginal bone resorption.[187]

Polyetheretherketone (PEEK) has been suggested as a material for abutments. This resin polymer is advantageous in chairside customization and gingival aesthetics, compared to metal abutments.[161] A previous animal experiment showed soft tissue quality around PEEK abutments similar to that around Ti.[188] Similar soft and hard tissue responses were also found in a previous randomized controlled trial comparing PEEK abutments with Ti.[189] However, such a polymer abutment is provisional, which is used as a healing abutment for a short period.[161,190]

Nowadays, the main materials used for abutments are Ti and zirconia (Fig. 9C). Traditionally, only Ti was used, but zirconia was developed for esthetic reasons due to the metallic color of Ti. A recent systematic review concluded that zirconia

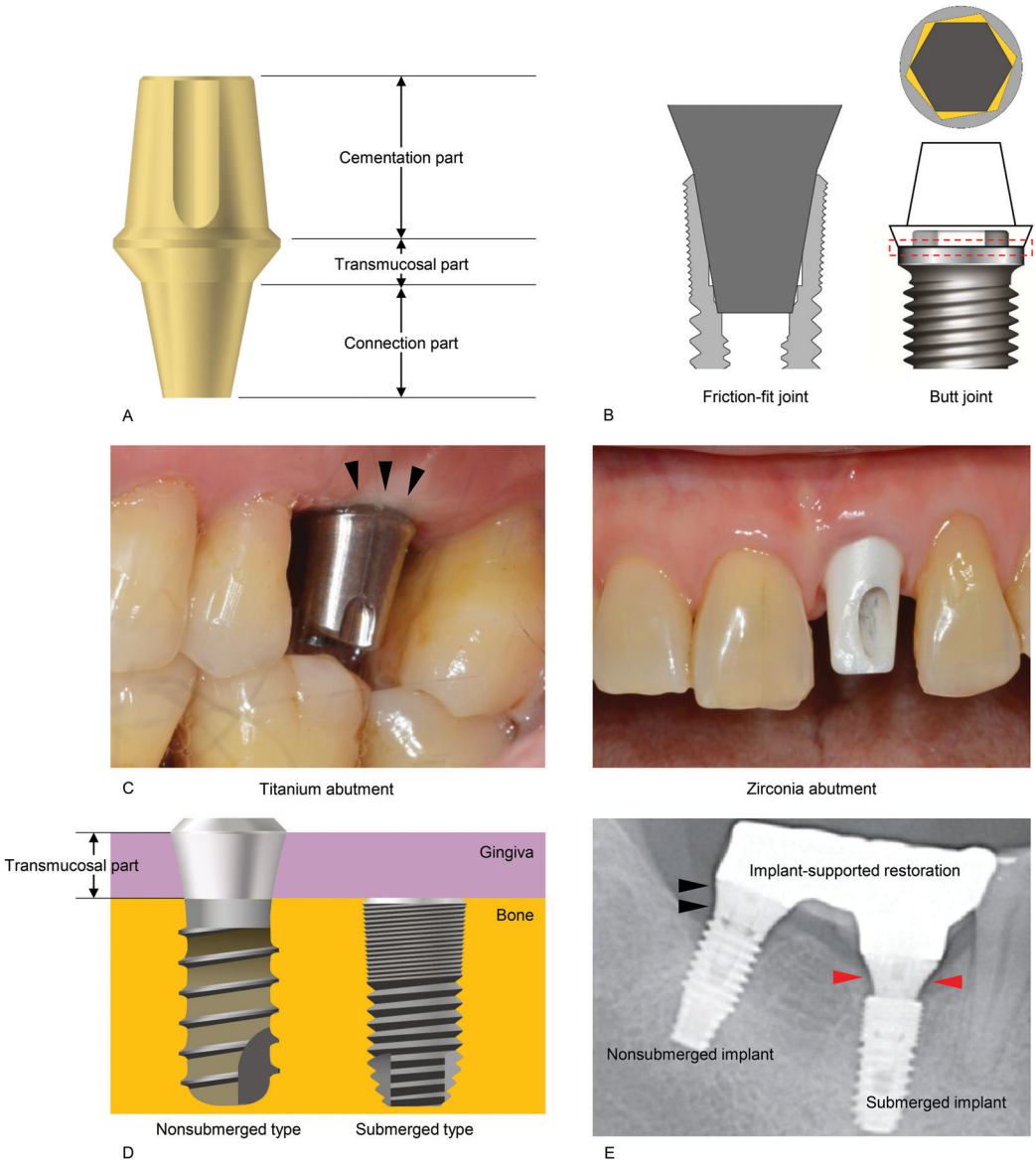

Fig. 9 (A) Three structures of an abutment, showing cementation, transmucosal, and connection areas. An artificial crown is cemented to the cementation part. The soft tissue seal is formed at the transmucosal area. The connection surface interfaces the surface of an implant (here, the inner surface). (B) Friction-fit joint (left) and butt joint (right). The top view shows the red dashed rectangular area in the diagram above, while the yellow area shows the machining tolerance allowing the possible movement of the abutment. (C) Titanium (left) *versus* zirconia (right) abutments. Note that the metal shade of titanium is reflected through the gingiva (black arrowheads). (D) Schematic diagram of a nonsubmerged implant (left) and a submerged implant (right). In the nonsubmerged implant, the transmucosal part forms an interface with the gingiva. (E) X-ray image showing the transmucosal collar (black arrowheads) around the implant in a nonsubmerged implant system, whereas the abutment (red arrowheads), rather than the implant, has a transmucosal layer in a submerged system.

abutments are more advantageous as they cause less discoloration of the soft tissue than Ti abutments.[191] In addition, a previous meta-analytic study described that zirconia abutments showed less bacterial adhesion, less plaque retention and less soft tissue inflammation than Ti.[192] In terms of the soft tissue seal, however, there is abundant evidence that there are no significant differences between the two materials;[186,187,193] furthermore, zirconia has a lower fracture strength than Ti, and hence, Ti is still widely used in abutments. If a zirconia abutment is used, the high fracture rate can disrupt the soft tissue seal. Clinically, it is possible to overcome the esthetic problem of the color of Ti with a bone graft, a soft tissue graft, and modification of the prosthesis. A recent meta-analysis of spectrophotometric evaluation has revealed that there was no clear evidence supporting the superiority of zirconia abutments in peri-implant soft tissue color, compared to Ti abutments.[194]

3.3.3. Abutment dis-/re-connection. When an abutment is disconnected, intraoral bacteria can penetrate into the peri-implant soft tissue or hard tissue, leading to marginal bone resorption. During prosthodontic procedures and/or clinical maintenance, abutments are occasionally disconnected and reconnected. Previous human and *in vivo* studies showed that

the marginal bone level was maintained when the frequency of abutment dis- and re-connection was minimized.[195–198] This abutment dis-/re-connection procedure compromised the soft tissue seal, eventually causing marginal bone resorption[199] Some clinicians have suggested a 'one abutment-one time' concept, to prevent marginal bone resorption *via* this route.[198,200]

3.3.4. Effects of surface treatments on abutment. The soft tissue seal is among the most important factors contributing to the longevity of implant-supported restorations. Methods for abutment surface modification to strengthen the soft tissue attachment are similar to those for implant surface modification to improve the hard tissue integration. Micro- and nanotechnology have been applied to the transmucosal surface of the abutment to enhance the soft tissue seal.[161,201,202] Various surface treatments can alter the surface topography or characteristics, including machining, blasting, plasma spraying, chemical or electrochemical etching, laser treatment, and others.[161]

Some animal studies revealed higher attachment of connective tissue on a laser-grooved Ti abutment, when compared to the turned smooth-surfaced Ti abutment.[203–205] The connective tissue fibers were perpendicularly oriented to this laser-treated abutment, which is more protective against bacterial invasion.[206] A Ti abutment treated by oxidation also showed the improved soft tissue seal in another previous animal study, when compared to the turned smooth-surfaced Ti abutment.[207] Thus, in terms of surface roughness, the soft tissue seal may be improved when the abutment surface is rougher, although some studies are found to fail in detecting significant differences between modified rough and turned smooth abutment surfaces in soft tissue attachment.[208,209] This is because rougher surfaces provide a greater available surface area for soft tissue to attach.[210]

Nanotechnologically, photofunctionalization by ultraviolet rays, coating cell adhesive molecules including poly-L-lysine and nanoporous modification of abutment surfaces were also reported to strengthen the soft tissue seal around the abutments.[201,202,211] In one *in vitro* study, Yang *et al.* showed that gingival fibroblasts proliferate more strongly on smooth or rough zirconia surfaces following ultraviolet irradiation.[212] Epithelial attachment was also improved on both the abutment surfaces with poly-L-lysine coating and with laser-induced micro- or nano-pores that were within 5 μm in diameter.[201,202]

Abutment surface modification can improve the soft tissue seal. However, more plaque may accumulate on treated surfaces when the seal is broken. Modification of the abutment surface usually changes the surface roughness or surface free energy, which may increase the probability of bacterial colonization.[213–215] Furthermore, an unstable implant–abutment connection can make a modified abutment surface ineffective in the tight seal of soft tissue because such an instability allows abutment movement during mastication.[5,182] Clinical investigations are lacking and are needed to verify the effect of abutment surface treatment on the soft tissue seal, which safe-guards the implant from bacterial invasion and peri-implantitis.[202]

3.3.5. Implant systems with non-submerged structures. Although this review explores two major implant–abutment connection structures employed in the clinic, another implant system, the so-called nonsubmerged type implant, should also be discussed with respect to the soft tissue seal. When the top of the implant is positioned at the level of the gingival margin, the implant is classified as a nonsubmerged type (Fig. 9D).[216] The two implant–abutment connections (butt joint and friction-fit joint) are classifications in the submerged implant system, where the top of the implant is located at the level of alveolar bone. The soft tissue seal forms on part of the abutment in submerged type implants, and on the neck portion of an implant in nonsubmerged type implants (Fig. 9D).[5] Nonsubmerged implants are designed to stabilize the soft tissue seal; the transmucosal area is part of the implant (Fig. 9E). Therefore, abutment movement does not disturb the soft tissue seal, resulting in marginal bone preservation;[182,217] however, nonsubmerged implants are unable to effectively transfer stress or masticatory load, which is concentrated at the bone crestal area, leading to marginal bone resorption.[166,218] Clinically, the nonsubmerged design limits reproduction of the patient's emergence profile, making it very difficult to provide natural-looking implant-supported prostheses for long-term clinical service.[219]

Histologically, there are no significant differences between nonsubmerged and submerged implants; the type and extent of soft tissue attachment are similar.[220] The amount of soft tissue seal is 3 to 4 mm in an implant site; hence, the height of this part should be at least 3 mm.[221] When the height is less than 3 mm, which often occurs on deep insertion of a nonsubmerged implant, marginal bone resorption can occur to accomplish 3 mm of soft tissue seal.[219] The transmucosal collar of a nonsubmerged implant is usually machined to be smooth. Recently, there have been many attempts to reinforce the soft tissue attachment, such as by roughening the transmucosal area, or adding microgrooves to the transmucosal surface by laser treatment.[203,210,215,222–225] Connective tissue fibers are reported to perpendicularly adhere to microgrooved surfaces, which are more resistant to inflammatory infiltration;[226] however, these modifications increase biofilm formation on the surface, resulting in a more inflammatory environment around the implants.[215,222]

4. The implant–abutment interface: mechanical properties provoking pathogenesis

The success of dental implant treatment depends on many factors affecting the implant–abutment interface as well as the implant–bone and abutment–soft tissue interfaces.[158,159,175] One of the most frequent complications in the field of clinical implantology is loosening of the abutment screw between an implant and abutment, which may result in peri-implantitis.[177,227] This complication can lead to implant failure. Therefore, it is necessary to understand the implant–abutment interface, consisting of an implant, abutment, and abutment screw.

4.1. Biomechanics at the implant–abutment interface

In general, stability of the implant–abutment connection is essential for the long-term clinical success of a dental

implant.[5,48,158] To effectively tackle complications arising from unstable implant–abutment connection, which can occur on a daily basis, we must comprehend the biomechanics at the implant–abutment interface. Herein, we discuss the biomechanics of the two implant–abutment connections most widely used in the global dental implant industry: screw-retained only (SR) and friction-screw-retained (FSR).

4.1.1. Butt-jointed interface: retaining the implant–abutment connection using only a screw. The SR connection attaches implants and abutments using only an abutment screw (Fig. 10A). In clinical dentistry, this type of joint is referred to as an external hex connection because the shape of the implant top is hexagonal (Fig. 10A). The flat surface of the implant top is in direct contact with that of the abutment base, hence this connection has a butt joint interface (Fig. 10A). SR connections are stabilized only by tightening the abutment screw, which causes elongation of the screw and generates preload. Preload is an important variable in screw mechanics, as connection stability depends on screw-preload, which functions as a clamping force for the implant–abutment assembly, providing joint stability between the implant and the abutment.[163,228]

Some of the terms used in screw mechanics are illustrated in Fig. 10B. All screw components of implant systems discussed here have single threads (*i.e.*, the lead, l, of the screw is the same as its pitch, P). The biomechanics of the SR connection can be theoretically analyzed using screw mechanics with a free body diagram (Fig. 10B). Acceleration is zero when torque is applied to a screw just before it rotates. The equilibrium of force for the horizontal axis (F_H) is expressed using the following equation:[163]

$$F_H = -A\sin\phi + B\cos\phi - \mu N = 0 \quad (1)$$

where A is the preload, B is the transitional force due to torque, N is the normal force occurring between two frictional threads, μ is the friction coefficient between the threads, and ϕ is the lead angle of the screw. The normal force (N) is

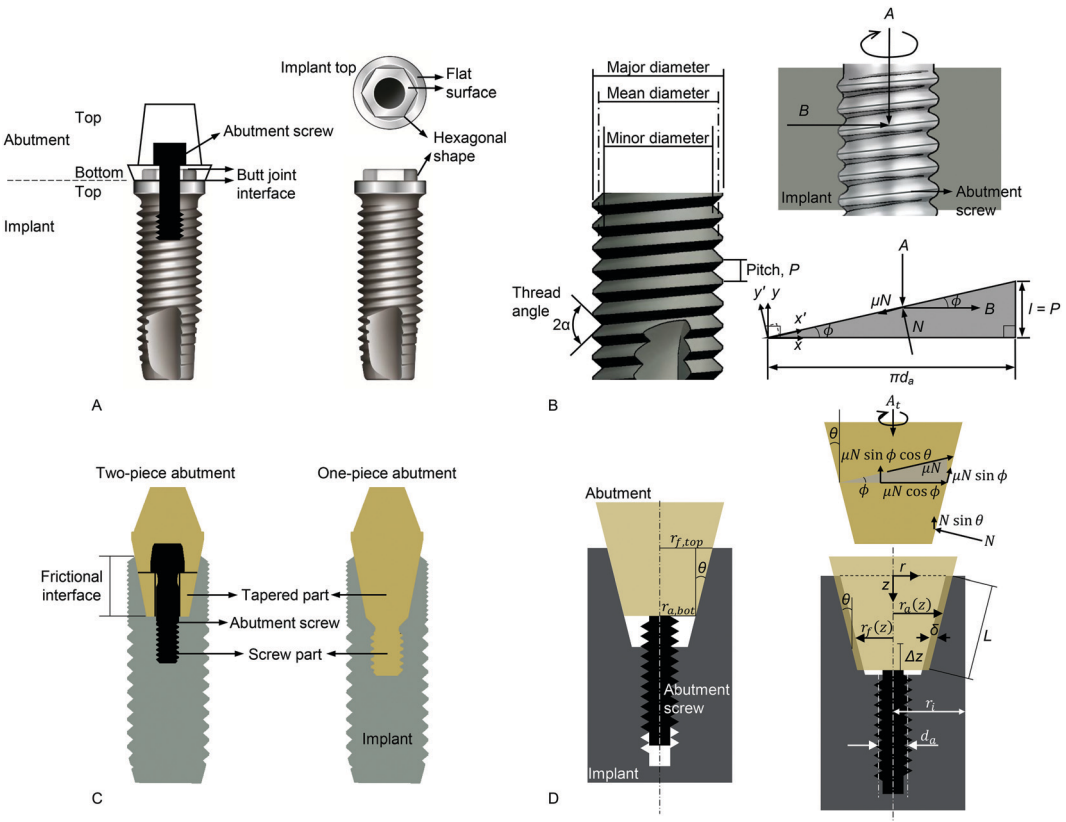

Fig. 10 (A) The SR connection structure in dental implants. This diagram shows why the connection is called an external hex connection in clinical dentistry. The abutment covers the hexagonal part of the implant top area. Notably, the butt joint is made between the flat surfaces of the implant and abutment. (B) Terms and diagrams for screw mechanics. The major diameter is defined as the largest diameter of a screw thread, and the minor diameter is the smallest diameter. The mean diameter is the average diameter of a screw, which is, strictly, not the mean of the major and minor diameters. When the abutment screw is tightened, a preload, A, is generated. All screws in this section are right-handed. A free body diagram, or force analysis, is shown in the lower right corner. (C) The FSR connection structure in dental implants. A two-piece (left) and one-piece (right) abutment are shown. Note that the tapered and screw parts are fused into a single body in the one-piece abutment, which implies that a decrease in preload in the screw part would have a stronger effect on the tapered part, compared with a two-piece abutment. (D) Diagrams depicting friction mechanics in the FSR connection.[159] (Reproduced from ref. 159 with permission from Elsevier.) On the left, the abutment is placed in the implant with no interference. Tightening causes the abutment to engage tightly into the implant with interference (δ), shown on the lower right. Friction and preload occur between the interfaces, and contribute to the stability of the FSR implant–abutment connection. The free body diagram (upper right) is shown at the tapered or conical area.

$$N = A\cos\phi + B\sin\phi \quad (2)$$

Combining (1) with (2), we get

$$B\cos\phi - A\sin\phi = \mu(A\cos\phi + B\sin\phi) \quad (3)$$

Using eqn (3), the tightening torque, $\tau_{t,screw}$, is calculated as follows:

$$\tau_{t,screw} = \frac{d_a}{2}B = \frac{d_a}{2}A\frac{\tan\phi + \mu}{1 - \mu\tan\phi} \quad (4)$$

where d_a is the mean screw diameter.[163] For a typical 'V-shaped' thread with a thread angle 2α, the frictional terms in eqn (4) must be divided by $\cos\alpha$.[229] Therefore, if $\tan\phi = \frac{l}{\pi d_a}$ is applied to eqn (4), eqn (5) becomes

$$\tau_{t,screw} = \frac{d_a}{2}A\frac{l + \pi\mu_k d_a \sec\alpha}{\pi d_a - \mu_k l\sec\alpha} \quad (5)$$

where μ_k is the kinetic friction coefficient.[159] Screw tightening is usually considered a dynamic process. When the screw is loosened, a force is applied in the opposite direction. Therefore, the transitional force is $-B$ and the frictional force is $+\mu N$.[163] Modifying eqn (5) to account for the force equilibrium when loosening torque is applied gives

$$\tau_{l,screw} = \frac{d_a}{2}A\frac{\pi\mu_s d_a \sec\alpha - l}{\pi d_a + \mu_s l\sec\alpha} \quad (6)$$

where μ_s is the static friction coefficient, which considers the onset of screw loosening; however, the friction coefficient can be assumed to remain unchanged, because screws are essentially static at both the immediate cessation of tightening and the start of loosening.[163] Herein, we have derived the equations under the assumption that the kinetic and static friction coefficients are equal, that is, $\mu_k = \mu_s = \mu$.

The difference in torque between tightening and loosening is linearly calculated from a simple equation, since ϕ and $\mu\sec\alpha$ are very small values.[163]

$$\Delta\tau = \tau_t - \tau_l = A\frac{l}{\pi} \quad (7)$$

when the abutment screw is made of grade 5 Ti, the Ti yield strength is approximately 827 MPa. Therefore, the required preload against screw loosening was evaluated as >620 MPa (75% of the yield strength).[230,231] The thread depth of the abutment screws was approximately 0.2 mm, the major diameter was 2.0 mm, and three to five threads were engaged in tightening.[163] Therefore, the calculated preloads, converted to the pressure unit, MPa, ranged from 43.2 to 124.2 MPa. All predicted preloads were below the required level of 620 MPa. From eqn (7) and the linear model reported in a previous study, to prevent screw loosening, the tightening torque of an abutment screw should be >200 N cm, which is unrealistic and unachievable without mechanical or biological failures, including abutment screw fracture and bone disintegration from implants.[163]

This analytical approach indicates that the torque clinically recommended by the manufacturers, of 30–35 N cm, was actually insufficient to prevent screw loosening events. In clinical terms, this indicates that abutment screws should be repeatedly retightened in the SR connection for butt-joint interfaces between abutments and implants. Another important point raised by these studies is that features other than screws are needed to continuously maintain the implant–abutment connection. An interface stabilized by friction is one option, and is described below.

4.1.2. Frictional interface: retaining the implant–abutment connection using friction and a screw. The stability of the FSR connection structure is maintained by tight contact between the inner surface of an implant and the outer surface of an abutment, as well as an abutment screw (Fig. 10C). Friction occurs at this tight contact, which contributes significantly to the implant–abutment connection.[159] In clinical dentistry, this type of joint is called an internal friction connection, because it has a frictional interface, and the abutment is inserted into the inner part of the implant when connected (Fig. 10C).[5] As shown in Fig. 10C, a one-piece abutment has a frictional tapered part fused to the screw part, while a two-piece abutment consists of a tapered part and a separate abutment screw. The tightening process causes interference in the tapered part and advances the screw to generate preload.

When the implant and the abutment are made of the same material, the biomechanics of the FSR connection between the conical (tapered) and screw parts are analyzed separately.[159] The total tightening torque, $\tau_{t,total}$, is the sum of the torque values of the conical and screw parts:

$$\tau_{t,total} = \tau_{t,cone} + \tau_{t,screw} \quad (8)$$

Fig. 10D shows schematic diagrams of the conical part engaged into the implant. In the equilibrium state, the FSR connection is stable, as occurs at the cessation of tightening. The same friction coefficient, μ, can be used for both tightening and loosening. On the left of Fig. 10D, the bottom of the abutment is located at $z = (r_{f,top} - r_{a,bot})/\tan\theta$ when the abutment is placed in the implant with no interference. The tightening procedure induces a vertical force and the abutment tightly engages into the implant with interference, as shown in Fig. 10D (right). Interference, δ, and contact length, L, are calculated as follows:[228]

$$\delta = \Delta z\tan\theta \quad (9)$$

$$L = \frac{(r_{f,top} - r_{a,bot})}{\sin\theta} + \Delta z/\cos\theta \quad (10)$$

The interference applies pressure to the implant–abutment interface, and this contact pressure, denoted as p, is calculated as

$$p(z) = \frac{E\delta\left[r_i^2 - r_a^2(z)\right]\cos\theta}{2r_a(z)r_i^2} \quad (11)$$

along the vertical distance from the implant top, z.[228] E is Young's modulus of the implant or abutment material (equal) and r_i is the radius of the implant. The tapered outer radius of the abutment, $r_a(z)$, and the tapered inner radius of the implant, $r_f(z)$, vary along z according to the equations

$$r_a(z) = r_{a,bot} + (L\cos\theta - z)\tan\theta \quad (12)$$

$$r_f(z) = r_{f,top} - z\tan\theta \quad (13)$$

The differential, dN, of the normal force, N, is calculated along z as follows:

$$dN = p(z) \times 2\pi r_a(z)dz \quad (14)$$

Therefore, when ϕ is the lead angle of the screw, the tightening torque at the conical area, $\tau_{t,cone}$, is as follows:[159]

$$\begin{aligned}\tau_{t,cone} &= \int d\tau = \int r_a(z)\mu dN\cos\phi \\ &= 2\pi\mu\int_0^{L\cos\theta} {r_a}^2(z)p(z)dz\cos\phi \\ &= \frac{\pi\mu EL\Delta z\sin 2\theta\cos\phi}{8r_i^2}\left[L\sin\theta\left\{2\left(r_i^2 - 3{r_{a,bot}}^2\right)\right.\right. \\ &\quad \left.\left. - L\sin\theta\left(4r_{a,bot} + L\sin\theta\right)\right\} + 4r_{a,bot}\left(r_i^2 - {r_{a,bot}}^2\right)\right]\end{aligned} \quad (15)$$

The total tightening torque, $\tau_{t,total}$, is obtained by combining eqn (5), (8), and (15)

$$\begin{aligned}\tau_{t,total} &= \frac{d_a}{2}A_t\frac{l + \pi\mu d_a\sec\alpha}{\pi d_a - \mu l\sec\alpha} + \frac{\pi\mu EL\Delta z\sin 2\theta\cos\phi}{8r_i^2} \\ &\quad \times \left[L\sin\theta\left\{2\left(r_i^2 - 3{r_{a,bot}}^2\right) - L\sin\theta\left(4r_{a,bot} + L\sin\theta\right)\right\}\right. \\ &\quad \left. + 4r_{a,bot}\left(r_i^2 - {r_{a,bot}}^2\right)\right]\end{aligned} \quad (16)$$

where the preload, A_t, is calculated as $A_t = N\sin\theta + \mu N\sin\phi\cos\theta$ (Fig. 10D).[159]

Total loosening torque can also be analyzed in the same way. The preload becomes $A_l = N\sin\theta - \mu N\sin\phi\cos\theta$ at loosening, because the vector of friction is opposite to the direction at tightening. The loosening torque, $\tau_{l,cone}$, gives the same result at the conical part from eqn (14):[159]

$$\begin{aligned}\tau_{l,cone} &= \frac{\pi\mu EL\Delta z\sin 2\theta\cos\phi}{8r_i^2}\left[L\sin\theta\left\{2\left(r_i^2 - 3{r_{a,bot}}^2\right)\right.\right. \\ &\quad \left.\left. - L\sin\theta\left(4r_{a,bot} + L\sin\theta\right)\right\} + 4r_{a,bot}\left(r_i^2 - {r_{a,bot}}^2\right)\right]\end{aligned} \quad (17)$$

Using eqn (6) and (17), the total loosening torque, $\tau_{l,total} = \tau_{l,cone} + \tau_{l,screw}$, is

$$\begin{aligned}\tau_{l,total} &= \frac{d_a}{2}A_l\frac{\pi\mu d_a\sec\alpha - l}{\pi d_a + \mu l\sec\alpha} + \frac{\pi\mu EL\Delta z\sin 2\theta\cos\phi}{8r_i^2} \\ &\quad \times \left[L\sin\theta\left\{2\left(r_i^2 - 3{r_{a,bot}}^2\right) - L\sin\theta\left(4r_{a,bot}\right.\right.\right. \\ &\quad \left.\left.\left. + L\sin\theta\right)\right\} + 4r_{a,bot}\left(r_i^2 - {r_{a,bot}}^2\right)\right]\end{aligned} \quad (18)$$

Note that eqn (18) is applied until the onset of loosening. After the screw part is loosened, preload ceases, hence $\tau_{l,screw} = 0$, and only $\tau_{l,cone}$ remains in eqn (18).[159] If we consider this physical phenomenon associated with the separate parts of an abutment and an abutment screw (2-piece abutment), it is more easily understandable.

Eqn (16) and (18) predict various biomechanical properties for FSR connections. Notably, the magnitudes of both torques depend on the contact length, L, in a four-powered manner (*i.e.*, L^4). A slight increase in contact length results in a huge increase in loosening torque, clearly stabilizing the implant–abutment connection. When an implant and abutment are made of grade 4 commercially pure Ti, using the other parameters of the FSR connection listed in Table 1, a graph of the loosening torque *versus* the contact length can be plotted (Fig. 11).

When the contribution quotient of the FSR connection is defined as the ratio of torque at the conical part to the total torque, the quotient is >0.8, which implies that the conical part of the FSR connection is a major contributor to implant–abutment connection stability.[159] Regarding the loosening procedure, the screw part is unable to stabilize the FSR connection after the onset of loosening, because the screw preload vanishes. Therefore, the contribution quotient is 1; only the conical part contributes to the FSR connection.[159] This frictional tapered part acts as an alternative stabilizer for implant–abutment connection when the preload of the screw part diminishes, especially for 2-piece abutments.

From eqn (16) and (18), loosening torque is linearly proportional to tightening torque. Subsequently, the screw preload

Table 1 FSR connection parameters[a]

Taper angle (θ)	11°
Frictional coefficient (μ, $\mu_s = \mu_k$)	0.3
Contact length (L)	2.228 mm
Half of the major diameter of the fixture (r_i)	2.205 mm
Δz	5 μm
Bottom radius of the abutment ($r_{a,bot}$)	1.427 mm
Young's modulus (grade 4 Ti)	113.8 GPa
Mean diameter of the abutment screw (d_a)	1.74 mm
Lead length of the abutment screw (l)	0.4 mm
Lead angle of the abutment screw (ϕ)	4.19°
Thread angle (2α)	60°

[a] Parameters are not exact values, they are taken from the literature.[159,163,228]

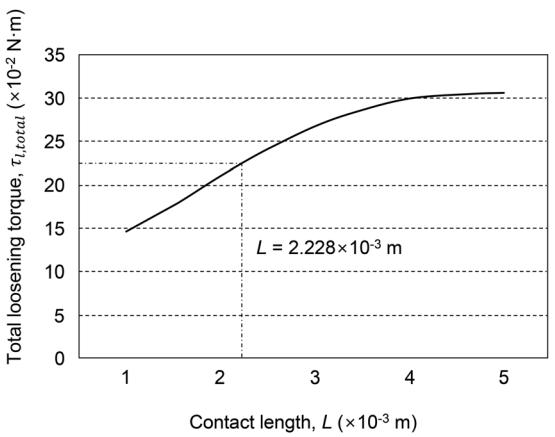

Fig. 11 The effect of contact length, L, on the total loosening torque, $\tau_{l,total}$. This graph shows total loosening torque values, based on the data in Table 1.

is linearly proportional to tightening torque. These linear relations are discussed above, and have been demonstrated both theoretically and experimentally.[163] Importantly, torque, preload, and implant–abutment stability are strongly affected by the interfacial frictional coefficient. Roughening or smoothening technologies at micro- or nano-scale to control the frictional coefficient can be crucial for implant–abutment stability, which is a key factor for biological and inflammatory responses around dental implants.

4.2. Control of the implant–abutment interface

To ensure the longevity of implant restorations, dental clinicians should seek to avoid any problems with the abutment, abutment screw, and prosthesis, by considering both mechanical and biological aspects of implant restoration. Mechanical complications include fracture or tearing of implants, fracture or loosening of an abutment screw, and fracture or dislodgement of a prosthesis (Fig. 12A).[232] Biological complications include problems in the osseointegrated bone and peri-implant mucosa, resulting from bacterial invasion (Fig. 12B).[232] Biological complications are divided into peri-implant mucositis and peri-implantitis, the equivalent of gingivitis and periodontitis, respectively, in natural teeth.[168] The onset and progression of peri-implant disease and periodontal disease are similar, indicating comparable bacterial composition.[233] Biological complications caused by bacteria and mechanical complications were previously considered independent, but recent studies have demonstrated that they are associated.[234–236]

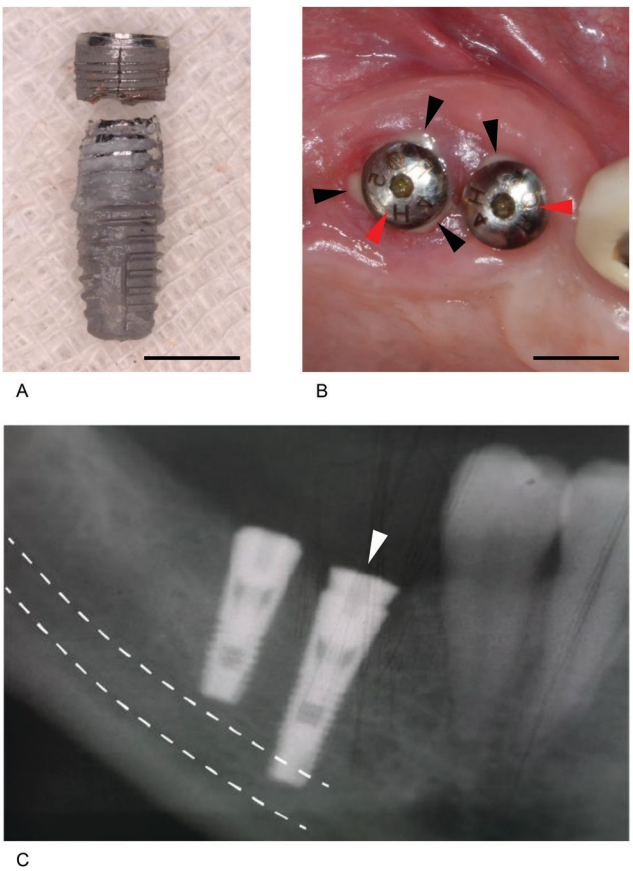

Fig. 12 Mechanical and biological complications of dental implants. (A) A fractured implant removed from the mouth of a patient. (B) Discharged yellowish pus (black arrowheads) found around the healing abutments (red arrowheads) connected to dental implants placed into the bone. (C) A long implant (white arrowhead) placed in the right mandibular first molar area invading the anatomical structure (the inferior alveolar canal; white dashed line), where the inferior alveolar nerve is located. Scale bars = 5 mm.

Disruption of the soft tissue seal is the main cause of peri-implant disease; detachment of the soft tissue seal allows colonization and invasion of bacteria, eventually leading to the peri-implant disease.[5] Destruction of the soft tissue seal around an implant can be driven by a lack of attached gingiva, shallowness of the vestibule, or a high frenum, but mainly results from movement of an abutment, due to a non-rigid and unstable connection between implant and abutment.[5,48,156] Therefore, mechanical joint stability between implant and abutment is a major factor determining the longevity of implant restorations.[48,158] There are several factors that contribute to a stable connection between implant and abutment.[48,158,159,163]

After delivery of a prosthesis, three kinds of force are applied to the implant-to-abutment interface: vertical, lateral, and rotational.[5] Physically, rotational force is a type of lateral or horizontal force. Most implant systems struggle with lateral force, but not vertical force, because the mating structures of the implant and abutment can tolerate vertical force.[5] Conversely, lateral force can loosen the abutment screw, making the abutment mobile. Essentially, the hexagonal male and female structures in each connecting part of an implant and an abutment are engineered to tolerate rotational force.[237] Therefore, in general, vertical, lateral, and rotational forces are supported by an implant–abutment mating structure, an abutment screw, and a hex structure.[5,238] For long-term successful results, an implant–abutment mating structure should endure and distribute these forces.[48,166,238]

The Brånemark implant system (Nobel Biocare, Zürich, Switzerland), the first marketed screw-shaped implant, is an example of an SR connection. In this system, the vertical force is endured by the platform of an implant and the mating abutment, while the lateral force is endured by the hex device and abutment screw, and the rotational force by the hex device.[238] This SR connection is a mobile structure, and occlusal forces are concentrated on an abutment screw.[237,238] Therefore, bacterial penetration is common, and peri-implant disease is likely to occur. To prevent movement of the abutment in this connection, the external hex feature should be lengthened, and the machining tolerance between female and male hex parts made more intimate. Alternatively, an abutment screw made from stronger materials can be incorporated, and the implant platform widened, to minimize the forces focused on the abutment screw. In addition, when a stronger tightening torque is applied, the strength of the connection is enhanced;[163] however, it is impossible to completely prevent movement of the abutment in this type of joint, because the external hex structures of the implants used clinically are approximately 0.7 mm in height, and therefore unable to maintain implant–

abutment connection stability under the stress of daily mastication (occlusal force).[5,237]

Many commercially popular implants have FSR connections, which also have an abutment screw, but this is less important than the butt joint in terms of stability.[159,166] Additionally, a few manufacturers produce implants without an abutment screw, in which the implant and abutment are held only through high friction between the two parts.[228,239] These joints have a 1.5° taper angle between the implant and abutment connection on one side, which locks the abutment and implant tightly, without an abutment screw.[239] This tight connection can bear vertical, horizontal, and rotational forces, rendering the abutment immobile, and thereby avoiding soft tissue seal disruption.[237] Therefore, marginal bone resorption rarely occurs with this system.[5,48,240] The degree of tapering of the abutment to the implant interface is a crucial factor in determining abutment mobility in the FSR connection; the wider the angle, the more unstable the abutment to implant connection, and the greater the need for an abutment screw.[159]

When an implant meets an abutment *via* the FSR connection, there is an intimate contact between them, initially at the connection surface, subsequently at the base, and then over the entire surface. This is because the implant top is gradually opened, causing the abutment to sink down, which loosens the abutment screw, leading to a need for periodic re-tightening.[175,241,242] Otherwise, abutment movement increases, leading to destruction of the soft tissue seal, and subsequent bacterial attack. Clinically, re-tightening can be performed several times if necessary.[243] Dental clinicians should understand the mechanics of the abutment to implant mating structure, and select products with a firm and stable connection, as well as an immobile abutment, to minimize the probability of peri-implant disease.

4.3. Clinical interpretation of soft and hard tissue responses around the implant–abutment interface

Artificial organs should perform similarly to their natural counterparts in the human body, and last for a long time. Indeed, longevity is becoming increasingly important as human lifespan increases. Dental implants must function as artificial organs to replace teeth and also persist in the oral cavity for a long time. Thus, mechanical failure of implants and the surrounding soft and hard tissue should be avoided for longevity to be achieved.

The anatomical structures surrounding an implant include the alveolar bone, the alveolar mucosa, and the gingiva. The alveolar bone meets the occlusal force applied to the implant, and the alveolar mucosa and gingiva protect the alveolar bone against oral bacteria (protective functions are mostly performed by the gingiva, but the alveolar mucosa contributes when the gingiva is absent or lacking).[148,244] The alveolar bone and gingiva are complementary to each other; gingival health is maintained by the lower alveolar bone, while the lower alveolar bone is protected by the upper gingiva.

It is considered a general rule that the alveolar bone responsible for mechanical masticatory force is resorbed by approximately 1–1.5 mm for the first year from the moment occlusal force is applied, and up to 0.2 mm per year may be lost thereafter.[245] This rule is based on implant success criteria from clinical analysis of the Brånemark system, but studies on mobile SR connections and rigid FSR connections have shown that alveolar bone may be preserved or even expanded after occlusal loading.[48,246–249] If first-year early loss and annual constant resorption of alveolar bone occurs after loading, long implants should be inserted to ensure long-term prognosis. In addition, bone grafts are needed to compensate for bone resorption before implantation. These bone grafts and placement of long implants can irritate patients and represent a challenge to surgeons, and long implants can occasionally invade anatomical structures, creating permanent disability for the patient (Fig. 12C). Accordingly, there is a trend toward implants that do not cause alveolar bone loss, which often occurs in implants with SR connections.[164,250,251]

Human alveolar bone is not resorbed in the presence of natural teeth; however, alveolar bone is destroyed by periodontitis, and this loss is almost irreversible.[252] Most of the alveolar bone is preserved, quantitatively and qualitatively, in the absence of periodontitis, except for small losses due to mechanical degeneration or aging.[253,254] This is due to appropriate stimulation by periodontal ligaments. Thus, time is spent predicting how the alveolar bone will change after implantation and loading. The quantity and quality of alveolar bone are not diminished in the absence of peri-implantitis, similar to periodontitis in natural teeth, and can be stimulated.[48,255]

The Astra Tech implant system (Dentsply Sirona Inc., Charlotte, NC, USA) was the first implant to embody this concept, and the specific action of the implant–abutment connection stimulates the alveolar bone, resulting in an absence of bone loss.[48] Frost's hypothesis can be applied to alveolar bone, as it can to other bone types.[16] Thus, osteoblasts are activated, and both the quantity and quality of alveolar bone are increased when an appropriate amount of strain is applied.[16,255]

Dental implants have been used in humans for many years, but most do not maintain a healthy state in the oral cavity after a long time.[256] As described above, biological and mechanical complications occur in implant-supported restorations.[256,257] Nevertheless, implants with SR connections perform better and have superior long-term prognosis, and these have gained widespread popularity since the 1980s.[258–261] The main difference between these implants and previous products is the presence or absence of threads. Previous products did not have a structure that could transfer the occlusal force to the alveolar bone, whereas implants with SR connections can transfer this load through the screw-shaped or threaded structure.[5] The thread at the surface of the implant transforms the shear stress generated at the interface between the implant and the alveolar bone into compressive stress, which allows the bone to tolerate the force.[5] These stresses also generate an appropriate strain on the alveolar bone that helps it to remain healthy in the long term.[16,158,238]

Nevertheless, micro-mobility in the implant–abutment connection causes marginal bone loss by destroying the mucosal seal formed by the gingiva.[5,158,182,237] The Brånemark implant

was the first to guarantee long-term prognosis, but has potential side effects, including marginal bone loss, resulting in patient suffering and challenges for dental clinicians, including performing bone-grafting and use of long implants.[262] Human alveolar bone is resorbed when bacterial invasion occurs or appropriate stimulation ceases.[5,16,263] Therefore, dental implants should stimulate the alveolar bone appropriately, without allowing bacterial invasion. Products based on this concept arrived on the market after implants with SR connections and implants with FSR connections have taken this concept further.[48,166,255]

In general, the abutment of implant systems with FSR connections is secured by an 11° conical connection to the inside of the implant, which converts the masticatory force into strain, stimulating the alveolar bone.[264] The occlusal load allows the abutment to slightly descend and press the implant inner wall.[5,175] When the implant region in contact with the marginal bone is expanded, strain occurs in the alveolar bone in the area, stimulating the alveolar bone, activating osteoblasts and increasing the quantity and quality of alveolar bone.[5] An increase in alveolar bone requires a significant change in the clinical procedure; if the quantity and quality of the alveolar bone increase significantly over time, the need for bone graft surgery is reduced, and a short implant can be clinically applied, to the satisfaction of both dental clinicians and patients.[255,262]

Marginal bone loss occurs in implants with mobile connections, which does not lead to immediate implant failure, but does create considerable problems from a periodontal standpoint.[164,182,256] Normally, these products dissolve the alveolar bone to the level of the first or second implant thread along the long axis.[245,265] Following the loss of alveolar bone, the upper gingiva may be lost or attached gingiva may become free.[5,148] Gingival loss, or transformation from attached to free gingiva, facilitates the invasion of oral bacteria, resulting in peri-implantitis.[156] Therefore, dental clinicians should closely monitor the condition of the marginal bone to ensure that the gingiva is sufficiently healthy and ensure good long-term prognosis. For the long-term clinical success of dental implants, stable implant–abutment connection is vital.[48,156] This immobile connection maintains a soft tissue seal, which is resistant to bacterial invasion, providing an environment favorable for alveolar bone preservation.[48,158,182,262]

5. Perspectives of future works and concluding remarks

Dental implants have been successfully used in the clinic for over 40 years; however, there are many potential mechanical and biological complications. A deeper understanding of dental implant systems is required to increase the probability of long-term clinical success when replacing a missing tooth, particularly given the increase in human lifespan. At first glance, mechanical complications of dental implant systems, such as screw loosening, appear to be independent of biological complications, such as peri-implantitis; however, these complications, which can lead to implant failure, are interconnected. A more profound comprehension of the three interfaces (bone–implant, gingiva–abutment, and implant–abutment) is gradually emerging and is definitely needed.

Hard tissue integration, or osseointegration, provided the first key breakthrough supporting the clinical success of dental implants. Surface modification can enhance bone healing and reinforce hard tissue integration at the bone–implant interface. Microtopography can modify the implant surface to mimic Howship's lacunae, which are bone-resorbed areas that stimulate bone deposition. Surface chemistry can also be altered to increase the interfacial bone contact, using inorganic elements or functional peptides. This approach could prove useful for treating edentulous patients with problems related to bone metabolism, although peptide-treated surfaces have not yet been clinically employed. The control of unexpected side effects is necessary before clinical use. Conjugation problems between biofunctional molecules and implant surfaces remain to be solved, particularly under the clinical situation of implant installation. Topographical or chemical modifications of implant surfaces will be continued in many ways as other materials including zirconia, as well as Ti, are being tried as implant materials. Topographical modification at microscale would go to make the implant surface more similar to the bone surface morphology. Nanotopographical surface modification would keep combined with various molecules showing therapeutic effects.

Discovering the soft tissue seal was another key breakthrough supporting clinical implant success. The epithelial and connective tissues should be firmly attached to an abutment surface, the characteristics and materials of which affect the attachment. When the soft tissue seal at the gingiva–abutment interface is broken, oral bacteria infiltrate and form biofilms, causing peri-implant inflammation that may result in clinical implant failure. Material development and surface treatment of abutments are under investigation for improved soft tissue seal and antibacterial effects. However, the quality of the soft tissue around an implant system is important for the soft tissue seal, with tender and mobile soft tissue being disadvantageous. Also, it should be noted that implant–abutment connection stability is another factor contributing to the seal.

The implant–abutment interface, comprising an implant, abutment, and abutment screw, should be sufficiently stable to maintain the soft tissue seal. Butt-jointed or SR connections are not resistant to preload loss, which is a natural phenomenon in screw mechanics. Therefore, the mobility of the implant–abutment connection increases with screw loosening, which breaks the soft tissue seal and causes the loss of peri-implant bone. Friction between the inclined planes of an abutment and an implant stabilizes the FSR connection, in addition to the abutment screw. These physical properties of the implant–abutment assembly reduce the mechanical complications of screw-loosening and fracture, which helps to maintain the soft tissue seal and assists in hard tissue integration. Such a comprehension of interfacial biomechanics leading to clinical phenomena will be helpful to researchers who develop future implants.

Author contributions

Jeong Chan Kim: conceptualization, investigation, resources, writing – original draft, visualization. Min Lee: validation, investigation, resources, writing – review and editing. In-Sung Luke Yeo: conceptualization, validation, investigation, resources, writing – original draft, writing – review and editing, visualization, supervision, project administration, funding acquisition.

Conflicts of interest

There are no conflicts to declare.

Acknowledgements

This work was supported by the National Research Foundation of Korea (NRF) grant funded by the Korea government (MSIT) (No. 2021R1A2C200465011).

References

1 *J. Prosthet. Dent.*, 2017, **117**(5S), e1–e105.
2 J. H. Jorge, C. C. Quishida, C. E. Vergani, A. L. Machado, A. C. Pavarina and E. T. Giampaolo, *J. Oral Sci.*, 2012, **54**, 337–342.
3 J. P. M. Tribst, A. M. O. Dal Piva, A. L. S. Borges, R. M. Araujo, J. M. F. da Silva, M. A. Bottino, C. J. Kleverlaan and N. de Jager, *Dent. Mater.*, 2020, **36**, 179–186.
4 C. J. Goodacre and W. P. Naylor, *Eur. J. Oral Implantol.*, 2016, **9**(suppl 1), S59–S68.
5 J. J. Kim, J. H. Lee, J. C. Kim, J. B. Lee and I. L. Yeo, *Materials*, 2019, **13**, 72.
6 T. Albrektsson, P. I. Brånemark, H. A. Hansson and J. Lindstrom, *Acta Orthop. Scand.*, 1981, **52**, 155–170.
7 I. L. Yeo, *Materials*, 2019, **13**, 89.
8 N. Meredith, *Int. J. Prosthodont.*, 1998, **11**, 491–501.
9 I. L. Yeo, *J. Dent. Oral. Biol.*, 2017, **2**, 1025.
10 A. M. Andreotti, M. C. Goiato, A. S. Nobrega, E. V. Freitas da Silva, H. G. Filho, E. P. Pellizzer and D. Micheline Dos Santos, *J. Periodontol.*, 2017, **88**, 281–288.
11 G. Zarb and T. Albrektsson, *Int. J. Periodontics Restorative Dent.*, 1991, **11**, 88–91.
12 T. Albrektsson, B. Chrcanovic, J. Molne and A. Wennerberg, *Eur. J. Oral Implantol.*, 2018, **11**(Suppl 1), S37–S46.
13 T. K. Kwon, J. Y. Choi, J. I. Park and I. L. Yeo, *Materials*, 2019, **12**, 1187.
14 I.-S. Yeo, in *Bone Response to Dental Implant Materials*, ed. A. Piattelli, Woodhead Publishing, Duxford, 2017, ch. 3, pp. 43–64.
15 H. Terheyden, N. P. Lang, S. Bierbaum and B. Stadlinger, *Clin. Oral. Implants Res.*, 2012, **23**, 1127–1135.
16 H. M. Frost, *Angle Orthod.*, 2004, **74**, 3–15.
17 N. A. Sims and J. H. Gooi, *Semin. Cell Dev. Biol.*, 2008, **19**, 444–451.
18 C. Gray, A. Boyde and S. J. Jones, *Bone*, 1996, **18**, 115–123.
19 T. Hefti, M. Frischherz, N. D. Spencer, H. Hall and F. Schlottig, *Biomaterials*, 2010, **31**, 7321–7331.
20 T. Albrektsson and A. Wennerberg, *Int. J. Prosthodont.*, 2004, **17**, 536–543.
21 M. Kulkarni, A. Mazare, E. Gongadze, S. Perutkova, V. Kralj-Iglic, I. Milosev, P. Schmuki, A. Iglic and M. Mozetic, *Nanotechnology*, 2015, **26**, 062002.
22 J. Y. Choi, J. H. Sim and I. L. Yeo, *J. Periodontal. Implant Sci.*, 2017, **47**, 182–192.
23 Y. S. Hong, M. J. Kim, J. S. Han and I. S. Yeo, *Implant Dent.*, 2014, **23**, 529–533.
24 J. W. Koh, Y. S. Kim, J. H. Yang and I. S. Yeo, *Int. J. Oral Maxillofac. Implants*, 2013, **28**, 790–797.
25 J. C. M. Souza, M. B. Sordi, M. Kanazawa, S. Ravindran, B. Henriques, F. S. Silva, C. Aparicio and L. F. Cooper, *Acta Biomater.*, 2019, **94**, 112–131.
26 J. Y. Choi, H. J. Lee, J. U. Jang and I. S. Yeo, *Implant Dent.*, 2012, **21**, 124–128.
27 A. Jemat, M. J. Ghazali, M. Razali and Y. Otsuka, *BioMed Res. Int.*, 2015, 791725.
28 T. K. Kwon, H. J. Lee, S. K. Min and I. S. Yeo, *Implant Dent.*, 2012, **21**, 427–432.
29 S. K. Min, H. K. Kang, D. H. Jang, S. Y. Jung, O. B. Kim, B. M. Min and I. S. Yeo, *BioMed Res. Int.*, 2013, 638348.
30 I. S. Yeo, S. K. Min, H. K. Kang, T. K. Kwon, S. Y. Jung and B. M. Min, *Biomaterials*, 2015, **73**, 96–109.
31 I. S. Yeo, S. K. Min, H. Ki Kang, T. K. Kwon, S. Y. Jung and B. M. Min, *Data Brief*, 2015, **5**, 411–415.
32 G. P. Freitas, H. B. Lopes, E. C. Martins-Neto, P. T. de Oliveira, M. M. Beloti and A. L. Rosa, *J. Oral Implantol.*, 2016, **42**, 240–247.
33 A. Barfeie, J. Wilson and J. Rees, *Br. Dent. J.*, 2015, **218**, E9.
34 A. Wennerberg, T. Albrektsson and B. Chrcanovic, *Eur. J. Oral Implantol.*, 2018, **11**(Suppl 1), S123–S136.
35 A. Wennerberg and T. Albrektsson, *Clin. Oral. Implants Res.*, 2009, **20**(Suppl 4), 172–184.
36 A. Gupta, M. Dhanraj and G. Sivagami, *Indian J. Dent. Res.*, 2010, **21**, 433–438.
37 M. Herrero-Climent, P. Lazaro, J. Vicente Rios, S. Lluch, M. Marques, J. Guillem-Marti and F. J. Gil, *J. Mater. Sci.: Mater. Med.*, 2013, **24**, 2047–2055.
38 C. B. Cho, S. Y. Jung, C. Y. Park, H. K. Kang, I. L. Yeo and B. M. Min, *Materials*, 2019, **12**, 3400.
39 J. Y. Choi, S. Kim, S. B. Jo, H. K. Kang, S. Y. Jung, S. W. Kim, B. M. Min and I. L. Yeo, *J. Biomed. Mater. Res. A*, 2020, **108**, 1214–1222.
40 S. Kim, J. Y. Choi, S. Y. Jung, H. K. Kang, B. M. Min and I. L. Yeo, *Int. J. Oral Maxillofac. Implants*, 2019, **34**, 836–844.
41 J. B. Lee, Y. H. Jo, J. Y. Choi, Y. J. Seol, Y. M. Lee, Y. Ku, I. C. Rhyu and I. L. Yeo, *Materials*, 2019, **12**, 2078.
42 I. Wall, N. Donos, K. Carlqvist, F. Jones and P. Brett, *Bone*, 2009, **45**, 17–26.
43 J. W. Park, T. G. Kwon and J. Y. Suh, *Clin. Oral. Implants Res.*, 2013, **24**, 706–709.
44 S. M. Li, W. H. Yao, J. H. Liu, M. Yu, L. Wu and K. Ma, *Surf. Coat. Technol.*, 2015, **277**, 234–241.

45 J. W. Wang, Y. Ma, J. Guan and D. W. Zhang, *Surf. Coat. Technol.*, 2018, **338**, 14–21.
46 L. Zhang, Y. Duan, R. Gao, J. Yang, K. Wei, D. Tang and T. Fu, *Materials*, 2019, **12**, 370.
47 P. G. Coelho, R. Jimbo, N. Tovar and E. A. Bonfante, *Dent. Mater.*, 2015, **31**, 37–52.
48 M. Donati, A. Ekestubbe, J. Lindhe and J. L. Wennström, *Clin. Oral. Implants Res.*, 2018, **29**, 480–487.
49 I. S. Yeo, *Open Biomed. Eng. J.*, 2014, **8**, 114–119.
50 M. Annunziata and L. Guida, *Front. Oral Biol.*, 2015, **17**, 62–77.
51 D. Buser, S. F. Janner, J. G. Wittneben, U. Brägger, C. A. Ramseier and G. E. Salvi, *Clin. Implant Dent. Relat. Res.*, 2012, **14**, 839–851.
52 L. Feller, R. Chandran, R. A. Khammissa, R. Meyerov, Y. Jadwat, M. Bouckaert, I. Schechter and J. Lemmer, *SADJ*, 2014, **69**(112), 114–117.
53 O. E. Ogle, *Dent. Clin. North Am.*, 2015, **59**, 505–520.
54 E. El Chaar, L. Zhang, Y. Zhou, R. Sandgren, J. C. Fricain, M. Dard, B. Pippenger and S. Catros, *Int. J. Oral Maxillofac. Implants*, 2019, **34**, 443–450.
55 S. M. Hamlet, R. S. B. Lee, H. J. Moon, M. A. Alfarsi and S. Ivanovski, *Clin. Oral. Implants Res.*, 2019, **30**, 1085–1096.
56 L. Cigerim and V. Kaplan, *J. Oral Implantol.*, 2020, **46**, 475–479.
57 A. Markovic, A. Dinic, J. L. Calvo Guirado, A. Tahmaseb, M. Scepanovic and B. Janjic, *Clin. Oral. Implants Res.*, 2017, **28**, 1241–1247.
58 E. A. Bonfante, M. N. Janal, R. Granato, C. Marin, M. Suzuki, N. Tovar and P. G. Coelho, *Clin. Oral. Implants Res.*, 2013, **24**, 1375–1380.
59 H. K. Kang, O. B. Kim, S. K. Min, S. Y. Jung, D. H. Jang, T. K. Kwon, B. M. Min and I. S. Yeo, *Biomaterials*, 2013, **34**, 4027–4037.
60 S. Mei, F. Dong and M. S. Rahman Khan, *J. Oral Maxillofac. Surg.*, 2018, **76**, 2104.e1.
61 C. E. Oeschger, D. D. Bosshardt, S. Roehling, M. Gahlert, D. L. Cochran and S. F. M. Janner, *Clin. Oral Investig.*, 2020, **24**, 3609–3617.
62 E. Velasco-Ortega, A. Jimenez-Guerra, L. Monsalve-Guil, I. Ortiz-Garcia, A. I. Nicolas-Silvente, J. J. Segura-Egea and J. Lopez-Lopez, *Materials*, 2020, **13**, 1553.
63 P. Nicolau, F. Guerra, R. Reis, T. Krafft, K. Benz and J. Jackowski, *Quintessence Int.*, 2019, **50**, 114–124.
64 S. P. Hicklin, S. F. Janner, N. Schnider, V. Chappuis, D. Buser and U. Bragger, *Int. J. Oral Maxillofac. Implants*, 2020, **35**, 1013–1020.
65 T. Li, K. Gulati, N. Wang, Z. Zhang and S. Ivanovski, *Mater. Sci. Eng., C*, 2018, **88**, 182–195.
66 J. Park, S. Bauer, K. A. Schlegel, F. W. Neukam, K. von der Mark and P. Schmuki, *Small*, 2009, **5**, 666–671.
67 S. A. Alves, S. B. Patel, C. Sukotjo, M. T. Mathew, P. N. Filho, J. P. Celis, L. A. Rocha and T. Shokuhfar, *Appl. Surf. Sci.*, 2017, **399**, 682–701.
68 Y. C. Shin, K. M. Pang, D. W. Han, K. H. Lee, Y. C. Ha, J. W. Park, B. Kim, D. Kim and J. H. Lee, *Mater. Sci. Eng., C*, 2019, **99**, 1174–1181.
69 X. Miao, D. Wang, L. Xu, J. Wang, D. Zeng, S. Lin, C. Huang, X. Liu and X. Jiang, *Int. J. Nanomed.*, 2017, **12**, 1415–1430.
70 T. K. Ahn, D. H. Lee, T. S. Kim, G. C. Jang, S. Choi, J. B. Oh, G. Ye and S. Lee, *Adv. Exp. Med. Biol.*, 2018, **1077**, 355–368.
71 N. K. Awad, S. L. Edwards and Y. S. Morsi, *Mater. Sci. Eng., C*, 2017, **76**, 1401–1412.
72 C. Yin, Y. Zhang, Q. Cai, B. Li, H. Yang, H. Wang, H. Qi, Y. Zhou and W. Meng, *J. Biomed. Mater. Res. A*, 2017, **105**, 757–769.
73 G. Li, H. Cao, W. Zhang, X. Ding, G. Yang, Y. Qiao, X. Liu and X. Jiang, *ACS Appl. Mater. Interfaces*, 2016, **8**, 3840–3852.
74 S. Oh, K. S. Brammer, Y. S. Li, D. Teng, A. J. Engler, S. Chien and S. Jin, *Proc. Natl. Acad. Sci. U. S. A.*, 2009, **106**, 2130–2135.
75 X. Shen, P. Ma, Y. Hu, G. Xu, J. Zhou and K. Cai, *Colloids Surf., B*, 2015, **127**, 221–232.
76 M. K. Ji, G. Oh, J. W. Kim, S. Park, K. D. Yun, J. C. Bae and H. P. Lim, *J. Nanosci. Nanotechnol.*, 2017, **17**, 2312–2315.
77 C. G. Jothi Prakash, C. Clement Raj and R. Prasanth, *J. Colloid Interface Sci.*, 2017, **496**, 300–310.
78 L. M. Bjursten, L. Rasmusson, S. Oh, G. C. Smith, K. S. Brammer and S. Jin, *J. Biomed. Mater. Res. A*, 2010, **92**, 1218–1224.
79 N. Jiang, P. Du, W. Qu, L. Li, Z. Liu and S. Zhu, *Int. J. Nanomed.*, 2016, **11**, 4719–4733.
80 E. P. Su, D. F. Justin, C. R. Pratt, V. K. Sarin, V. S. Nguyen, S. Oh and S. Jin, *Bone Joint J.*, 2018, **100**, 9–16.
81 C. F. Ferreira, J. Babu, A. Hamlekhan, S. Patel and T. Shokuhfar, *Int. J. Oral Maxillofac. Implants*, 2017, **32**, 322–328.
82 Y. Li, Y. Song, A. Ma and C. Li, *BioMed Res. Int.*, 2019, 5697250.
83 C. Mu, Y. Hu, L. Huang, X. Shen, M. Li, L. Li, H. Gu, Y. Yu, Z. Xia and K. Cai, *Mater. Sci. Eng., C*, 2018, **82**, 345–353.
84 R. M. Sabino, J. V. Rau, A. De Bonis, A. De Stefanis, M. Curcio, R. Teghil and K. C. Popat, *Appl. Surf. Sci.*, 2021, **570**, 151163.
85 Z. Yuan, S. Huang, S. Lan, H. Xiong, B. Tao, Y. Ding, Y. Liu, P. Liu and K. Cai, *J. Mater. Chem. B*, 2018, **6**, 8090–8104.
86 H. G. Keceli, C. Bayram, E. Celik, N. Ercan, M. Demirbilek and R. M. Nohutcu, *J. Periodontal Res.*, 2020, **55**, 694–704.
87 Y. Zhang, L. Hu, M. Lin, S. Cao, Y. Feng and S. Sun, *ACS Omega*, 2021, **6**, 16364–16372.
88 K. Gulati and S. Ivanovski, *Expert Opin. Drug Delivery*, 2017, **14**, 1009–1024.
89 K. Gulati, J. C. Scimeca, S. Ivanovski and E. Verron, *Drug Discovery Today*, 2021, **26**, 2734–2742.
90 D. H. Kwon, S. J. Lee, U. M. E. Wikesjo, P. H. Johansson, C. B. Johansson and Y. T. Sul, *J. Clin. Periodontol.*, 2017, **44**, 941–949.
91 A. Hamlekhan, S. Sinha-Ray, C. Takoudis, M. T. Mathew, C. Sukotjo, A. L. Yarin and T. Shokuhfar, *J. Phys. D: Appl. Phys.*, 2015, **48**, 275401.
92 M. F. Kunrath, B. F. Leal, R. Hubler, S. D. de Oliveira and E. R. Teixeira, *AMB Express*, 2019, **9**, 51.

93 Y. Lin, L. Zhang, Y. Yang, M. Yang, Q. Hong, K. Chang, J. Dai, L. Chen, C. Pan, Y. Hu, L. Quan, Y. Wei, S. Liu and Z. Yang, *Stem Cells Int.*, 2021, 9993247.
94 K. S. Moon, Y. B. Park, J. M. Bae, E. J. Choi and S. H. Oh, *Materials*, 2021, **14**, 5976.
95 R. A. Ocampo and F. E. Echeverria, *Crit. Rev. Biomed. Eng.*, 2021, **49**, 51–65.
96 R. A. Gittens, L. Scheideler, F. Rupp, S. L. Hyzy, J. Geis-Gerstorfer, Z. Schwartz and B. D. Boyan, *Acta Biomater.*, 2014, **10**, 2907–2918.
97 M. Kulkarni, Y. Patil-Sen, I. Junkar, C. V. Kulkarni, M. Lorenzetti and A. Iglic, *Colloids Surf., B*, 2015, **129**, 47–53.
98 Y. Y. Go, J. Y. Mun, S. W. Chae, S. H. Kim, H. Song and J. J. Song, *Sci. Rep.*, 2018, **8**, 14581.
99 L. Sun, C. C. Berndt, K. A. Gross and A. Kucuk, *J. Biomed. Mater. Res.*, 2001, **58**, 570–592.
100 M. Xuereb, J. Camilleri and N. J. Attard, *Int. J. Prosthodont.*, 2015, **28**, 51–59.
101 B. A. van Oirschot, E. M. Bronkhorst, J. J. van den Beucken, G. J. Meijer, J. A. Jansen and R. Junker, *Clin. Oral. Implants Res.*, 2013, **24**, 355–362.
102 B. A. van Oirschot, E. M. Bronkhorst, J. J. van den Beucken, G. J. Meijer, J. A. Jansen and R. Junker, *Odontology*, 2016, **104**, 347–356.
103 K. Gotfredsen, A. Wennerberg, C. Johansson, L. T. Skovgaard and E. Hjørting-Hansen, *J. Biomed. Mater. Res.*, 1995, **29**, 1223–1231.
104 W. K. Yeung, G. C. Reilly, A. Matthews and A. Yerokhin, *J. Biomed. Mater. Res. B. Appl. Biomater*, 2013, **101**, 939–949.
105 N. Lopez-Valverde, A. Lopez-Valverde, J. M. Aragoneses, B. Macedo de Sousa, M. J. Rodrigues and J. M. Ramirez, *Materials*, 2021, **14**, 3015.
106 Z. Liu, X. Liu and S. Ramakrishna, *Biotechnol. J.*, 2021, **16**, e2000116.
107 L. Meirelles, A. Arvidsson, M. Andersson, P. Kjellin, T. Albrektsson and A. Wennerberg, *J. Biomed. Mater. Res. A*, 2008, **87**, 299–307.
108 V. C. Mendes, R. Moineddin and J. E. Davies, *J. Biomed. Mater. Res. A*, 2009, **90**, 577–585.
109 C. You, I. S. Yeo, M. D. Kim, T. K. Eom, J. Y. Lee and S. Kim, *Curr. Appl. Phys.*, 2005, **5**, 501–506.
110 J. Y. Choi, U. W. Jung, C. S. Kim, S. M. Jung, I. S. Lee and S. H. Choi, *Clin. Oral. Implants Res.*, 2013, **24**, 1018–1022.
111 J. Y. Choi, U. W. Jung, I. S. Lee, C. S. Kim, Y. K. Lee and S. H. Choi, *Clin. Oral. Implants Res.*, 2011, **22**, 343–348.
112 H. A. Acciari, D. P. S. Palma, E. N. Codaro, Q. Y. Zhou, J. P. Wang, Y. H. Ling, J. Z. Zhang and Z. J. Zhang, *Appl. Surf. Sci.*, 2019, **487**, 1111–1120.
113 I. S. Lee, B. Zhao, G. H. Lee, S. H. Choi and S. M. Chung, *Surf. Coat. Technol.*, 2007, **201**, 5132–5137.
114 E. T. Everett, *J. Dent. Res.*, 2011, **90**, 552–560.
115 J. E. Ellingsen, C. B. Johansson, A. Wennerberg and A. Holmen, *Int. J. Oral Maxillofac Implants*, 2004, **19**, 659–666.
116 J. E. Ellingsen, P. Thomsen and S. P. Lyngstadaas, *Periodontol.*, 2006, **41**, 136–156.
117 J. Y. Choi, S. H. Kang, H. Y. Kim and I. L. Yeo, *Int. J. Oral Maxillofac. Implants*, 2018, **33**, 1033–1040.
118 A. Wennerberg and T. Albrektsson, *Int. J. Oral Maxillofac. Implants*, 2010, **25**, 63–74.
119 M. Kassem, L. Mosekilde and E. F. Eriksen, *Eur. J. Endocrinol.*, 1994, **130**, 381–386.
120 S. F. Taxt-Lamolle, M. Rubert, H. J. Haugen, S. P. Lyngstadaas, J. E. Ellingsen and M. Monjo, *Acta Biomater.*, 2010, **6**, 1025–1032.
121 C. Mertens and H. G. Steveling, *Clin. Oral. Implants Res.*, 2011, **22**, 1354–1360.
122 G. Oxby, F. Oxby, J. Oxby, T. Saltvik and P. Nilsson, *Clin. Implant. Dent. Relat. Res.*, 2015, **17**, 898–907.
123 S. Windael, S. Vervaeke, L. Wijnen, W. Jacquet, H. De Bruyn and B. Collaert, *Clin. Implant. Dent. Relat. Res.*, 2018, **20**, 515–521.
124 R. Jimbo, R. Anchieta, M. Baldassarri, R. Granato, C. Marin, H. S. Teixeira, N. Tovar, S. Vandeweghe, M. N. Janal and P. G. Coelho, *Implant. Dent*, 2013, **22**, 596–603.
125 I. S. Yeo, J. S. Han and J. H. Yang, *J. Biomed. Mater. Res. B*, 2008, **87**, 303–311.
126 Z. Artzi, G. Carmeli and A. Kozlovsky, *Clin. Oral. Implants Res.*, 2006, **17**, 85–93.
127 A. Binahmed, A. Stoykewych, A. Hussain, B. Love and V. Pruthi, *Int. J. Oral Maxillofac. Implants*, 2007, **22**, 963–968.
128 G. Cannizzaro, P. Felice, A. Trullenque-Eriksson, M. Lazzarini, E. Velasco-Ortega and M. Esposito, *Eur. J. Oral Implantol.*, 2018, **11**, 163–173.
129 J. Mau, A. Behneke, N. Behneke, C. U. Fritzemeier, G. Gomez-Roman, B. d'Hoedt, H. Spiekermann, V. Strunz and M. Yong, *Clin. Oral. Implants Res.*, 2002, **13**, 477–487.
130 L. Sennerby and J. Roos, *Int. J. Prosthodont.*, 1998, **11**, 408–420.
131 S. K. Min, H. K. Kang, S. Y. Jung, D. H. Jang and B. M. Min, *Cell Death Differ.*, 2018, **25**, 268–281.
132 S. N. Stephansson, B. A. Byers and A. J. Garcia, *Biomaterials*, 2002, **23**, 2527–2534.
133 S. Y. Jung, O. B. Kim, H. K. Kang, D. H. Jang, B. M. Min and F. H. Yu, *Exp. Cell Res.*, 2013, **319**, 153–160.
134 J. J. Ryu, K. Park, H. S. Kim, C. M. Jeong and J. B. Huh, *Int. J. Oral Maxillofac. Implants*, 2013, **28**, 963–972.
135 F. Bohrnsen, J. Rublack, N. Aeckerle, A. Foerster, B. Schwenzer, J. Reichert, D. Scharnweber and H. Schliephake, *Int. J. Oral Maxillofac. Implants*, 2017, **32**, e175–e182.
136 S. Kim, C. Park, B. S. Moon, H. E. Kim and T. S. Jang, *J. Biomater. Appl.*, 2017, **31**, 807–818.
137 A. K. Shah, J. Lazatin, R. K. Sinha, T. Lennox, N. J. Hickok and R. S. Tuan, *Biol. Cell.*, 1999, **91**, 131–142.
138 J. D. Kang, *Spine J.*, 2011, **11**, 517–519.
139 D. S. Chan, J. Garland, A. Infante, R. W. Sanders and H. C. Sagi, *J. Orthop. Trauma*, 2014, **28**, 599–604.
140 E. J. Lytle, M. H. Lawless, G. Paik, D. Tong and T. M. Soo, *Spine J.*, 2020, **20**, 1286–1304.
141 B. C. Lee, I. S. Yeo, D. J. Kim, J. B. Lee, S. H. Kim and J. S. Han, *Clin. Oral. Implants Res.*, 2013, **24**, 1332–1338.

142 I. Jang, D. S. Choi, J. K. Lee, W. T. Kim, B. K. Cha and W. Y. Choi, *Biomed. Microdevices*, 2017, **19**, 94.
143 S. Ebara and K. Nakayama, *Spine*, 2002, **27**, S10–S15.
144 C. Stewart, B. Akhavan, S. G. Wise and M. M. M. Bilek, *Prog. Mater. Sci.*, 2019, **106**, 100588.
145 R. A. Latour, *Colloids Surf., B*, 2014, **124**, 25–37.
146 P. M. Bartold, L. J. Walsh and A. S. Narayanan, *Periodontol.*, 2000, **24**, 28–55.
147 T. Berglundh, J. Lindhe, I. Ericsson, C. P. Marinello, B. Liljenberg and P. Thomsen, *Clin. Oral. Implants Res.*, 1991, **2**, 81–90.
148 I. S. Moon, T. Berglundh, I. Abrahamsson, E. Linder and J. Lindhe, *J. Clin. Periodontol.*, 1999, **26**, 658–663.
149 I. Atsuta, Y. Ayukawa, A. Furuhashi, T. Yamaza, Y. Tsukiyama and K. Koyano, *J. Biomed. Mater. Res. A*, 2013, **101**, 2896–2904.
150 I. Atsuta, Y. Ayukawa, R. Kondo, W. Oshiro, Y. Matsuura, A. Furuhashi, Y. Tsukiyama and K. Koyano, *J. Prosthodont. Res.*, 2016, **60**, 3–11.
151 I. Atsuta, T. Yamaza, M. Yoshinari, T. Goto, M. A. Kido, T. Kagiya, S. Mino, M. Shimono and T. Tanaka, *Biomaterials*, 2005, **26**, 6280–6287.
152 T. G. Donley and W. B. Gillette, *J. Periodont.*, 1991, **62**, 153–160.
153 T. R. Gould, L. Westbury and D. M. Brunette, *J. Prosthet. Dent.*, 1984, **52**, 418–420.
154 H. Ikeda, M. Shiraiwa, T. Yamaza, M. Yoshinari, M. A. Kido, Y. Ayukawa, T. Inoue, K. Koyano and T. Tanaka, *Clin. Oral. Implants Res.*, 2002, **13**, 243–251.
155 H. Ikeda, T. Yamaza, M. Yoshinari, Y. Ohsaki, Y. Ayukawa, M. A. Kido, T. Inoue, M. Shimono, K. Koyano and T. Tanaka, *J. Periodont.*, 2000, **71**, 961–973.
156 S. Ivanovski and R. Lee, *Periodontol.*, 2018, **76**, 116–130.
157 G. E. Salvi, D. D. Bosshardt, N. P. Lang, I. Abrahamsson, T. Berglundh, J. Lindhe, S. Ivanovski and N. Donos, *Periodontol.*, 2015, **68**, 135–152.
158 J. H. Lee, J. C. Kim, H. Y. Kim and I. L. Yeo, *Int. J. Oral Maxillofac Implants*, 2020, **35**, 1195–1202.
159 D. Bozkaya and S. Müftü, *J. Biomech.*, 2005, **38**, 87–97.
160 C. A. A. Lemos, F. R. Verri, E. A. Bonfante, J. F. Santiago Junior and E. P. Pellizzer, *J. Dent.*, 2018, **70**, 14–22.
161 L. Canullo, M. Annunziata, P. Pesce, G. Tommasato, L. Nastri and L. Guida, *J. Prosthet. Dent.*, 2021, **125**, 426–436.
162 M. N. Abdallah, Z. Badran, O. Ciobanu, N. Hamdan and F. Tamimi, *Adv. Healthcare Mater.*, 2017, **6**, 1700549.
163 C. G. Jeong, S. K. Kim, J. H. Lee, J. W. Kim and I. S. L. Yeo, *Arch. Appl. Mech.*, 2017, **87**, 2003–2009.
164 S. Gracis, K. Michalakis, P. Vigolo, P. Vult von Steyern, M. Zwahlen and I. Sailer, *Clin. Oral. Implants Res.*, 2012, **23**(Suppl 6), 202–216.
165 B. Pardal-Pelaez and J. Montero, *J. Clin. Exp. Dent.*, 2017, **9**, e1355–e1361.
166 S. Hansson, *Clin. Oral. Implants Res.*, 2003, **14**, 286–293.
167 S. Kourtis, M. Damanaki, S. Kaitatzidou, A. Kaitatzidou and V. Roussou, *J. Esthet. Restor. Dent.*, 2017, **29**, 233–246.
168 J. G. Caton, G. Armitage, T. Berglundh, I. L. C. Chapple, S. Jepsen, K. S. Kornman, B. L. Mealey, P. N. Papapanou, M. Sanz and M. S. Tonetti, *J. Periodontol.*, 2018, **89**(Suppl 1), S1–S8.
169 M. G. Araujo and J. Lindhe, *J. Periodontol.*, 2018, **89**(Suppl 1), S249–S256.
170 T. Berglundh, G. Armitage, M. G. Araujo, G. Avila-Ortiz, J. Blanco, P. M. Camargo, S. Chen, D. Cochran, J. Derks, E. Figuero, C. H. F. Hammerle, L. J. A. Heitz-Mayfield, G. Huynh-Ba, V. Iacono, K. T. Koo, F. Lambert, L. McCauley, M. Quirynen, S. Renvert, G. E. Salvi, F. Schwarz, D. Tarnow, C. Tomasi, H. L. Wang and N. Zitzmann, *J. Periodontol.*, 2018, **89**(Suppl 1), S313–S318.
171 C. H. F. Hammerle and D. Tarnow, *J. Periodontol.*, 2018, **89**(Suppl 1), S291–S303.
172 L. J. A. Heitz-Mayfield and G. E. Salvi, *J. Periodontol.*, 2018, **89**(Suppl 1), S257–S266.
173 F. Schwarz, J. Derks, A. Monje and H. L. Wang, *J. Periodontol.*, 2018, **89**(Suppl 1), S267–S290.
174 S. Hurson, *Compend. Contin. Educ. Dent.*, 2018, **39**, 440–444, quiz 446.
175 J. H. Lee, Y. H. Huh, C. J. Park and L. R. Cho, *Int. J. Oral Maxillofac. Implants*, 2016, **31**, 1058–1065.
176 J. Torsten, *Clin. Implant Dent. Relat. Res.*, 2020, **22**, 226–236.
177 B. M. Vetromilla, L. P. Brondani, T. Pereira-Cenci and C. D. Bergoli, *J. Prosthet. Dent.*, 2019, **121**, 398–403.
178 D. Buser, L. Sennerby and H. De Bruyn, *Periodontol.*, 2017, **73**, 7–21.
179 I. Ericsson, L. G. Persson, T. Berglundh, C. P. Marinello, J. Lindhe and B. Klinge, *J. Clin. Periodontol.*, 1995, **22**, 255–261.
180 L. G. Persson, U. Lekholm, A. Leonhardt, G. Dahlen and J. Lindhe, *Clin. Oral. Implants Res.*, 1996, **7**, 90–95.
181 M. Quirynen, C. M. Bollen, H. Eyssen and D. van Steenberghe, *Clin. Oral. Implants Res.*, 1994, **5**, 239–244.
182 J. S. Hermann, J. D. Schoolfield, R. K. Schenk, D. Buser and D. L. Cochran, *J. Periodontol.*, 2001, **72**, 1372–1383.
183 J. Hadzik, U. Botzenhart, M. Krawiec, T. Gedrange, F. Heinemann, A. Vegh and M. Dominiak, *Ann. Anat.*, 2017, **213**, 78–82.
184 J. C. Kim, J. Lee, S. Kim, K. T. Koo, H. Y. Kim and I. L. Yeo, *J. Adv. Prosthodont.*, 2019, **11**, 147–154.
185 I. Abrahamsson, T. Berglundh and J. Lindhe, *Clin. Oral. Implants Res.*, 1998, **9**, 73–79.
186 M. Welander, I. Abrahamsson and T. Berglundh, *Clin. Oral. Implants Res.*, 2008, **19**, 635–641.
187 P. Serichetaphongse, W. Chengprapakorn, S. Thongmeearkom and A. Pimkhaokham, *Clin. Implant Dent. Relat. Res.*, 2020, **22**, 638–646.
188 M. Rea, S. Ricci, P. Ghensi, N. P. Lang, D. Botticelli and C. Soldini, *Clin. Oral. Implants Res.*, 2017, **28**, e46–e50.
189 T. Koutouzis, J. Richardson and T. Lundgren, *J. Oral Implantol.*, 2011, **37**(Spec No), 174–182.
190 M. Beretta, P. P. Poli, S. Pieriboni, S. Tansella, M. Manfredini, M. Cicciu and C. Maiorana, *Materials*, 2019, **12**, 3041.
191 D. Totou, O. Naka, S. B. Mehta and S. Banerji, *Int. J. Implant Dent.*, 2021, **7**, 85.

192 I. Sanz-Martin, I. Sanz-Sanchez, A. Carrillo de Albornoz, E. Figuero and M. Sanz, *Clin. Oral. Implants Res.*, 2018, **29**, 118–129.
193 R. J. Kohal, D. Weng, M. Bachle and J. R. Strub, *J. Periodontol.*, 2004, **75**, 1262–1268.
194 P. V. de Moura Costa, M. S. Ferreira, C. Verissimo, E. M. de Torres, J. Valladares-Neto and M. A. Garcia Silva, *Int. J. Oral Maxillofac. Implants*, 2021, **36**, 875–884.
195 I. Abrahamsson, T. Berglundh and J. Lindhe, *J. Clin. Periodontol.*, 1997, **24**, 568–572.
196 L. Canullo, Y. Omori, Y. Amari, G. Iannello and P. Pesce, *Clin. Implant Dent. Relat. Res.*, 2018, **20**, 668–673.
197 L. Canullo, P. Pesce, M. Tronchi, J. Fiorellini, Y. Amari and D. Penarrocha, *Clin. Implant Dent. Relat. Res.*, 2018, **20**, 976–982.
198 L. Canullo, I. Bignozzi, R. Cocchetto, M. P. Cristalli and G. Iannello, *Eur. J. Oral Implantol.*, 2010, **3**, 285–296.
199 Q. Q. Wang, R. Dai, C. Y. Cao, H. Fang, M. Han and Q. L. Li, *PLoS One*, 2017, **12**, e0186385.
200 M. Degidi, D. Nardi and A. Piattelli, *Clin. Oral. Implants Res.*, 2011, **22**, 1303–1307.
201 M. Contaldo, A. De Rosa, L. Nucci, A. Ballini, D. Malacrino, M. La Noce, F. Inchingolo, E. Xhajanka, K. Ferati, A. Bexheti-Ferati, A. Feola and M. Di Domenico, *Materials*, 2021, **14**, 3735.
202 B. Ghinassi, A. Di Baldassarre, G. D'Addazio, T. Traini, M. Andrisani, G. Di Vincenzo, G. Gaggi, M. Piattelli, S. Caputi and B. Sinjari, *Int. J. Mol. Sci.*, 2020, **21**, 6056.
203 G. Iglhaut, K. Becker, V. Golubovic, H. Schliephake and I. Mihatovic, *Clin. Oral. Implants Res.*, 2013, **24**, 391–397.
204 M. Nevins, M. Camelo, M. L. Nevins, P. Schupbach and D. M. Kim, *Int. J. Periodontics Restorative Dent.*, 2012, **32**, 385–392.
205 M. Nevins, D. M. Kim, S. H. Jun, K. Guze, P. Schupbach and M. L. Nevins, *Int. J. Periodont. Restor. Dent.*, 2010, **30**, 245–255.
206 R. Neiva, N. Tovar, R. Jimbo, L. F. Gil, P. Goldberg, J. P. Barbosa, T. Lilin and P. G. Coelho, *Int. J. Periodontics Restorative Dent.*, 2016, **36**, 673–679.
207 F. Teng, H. Chen, Y. Xu, Y. Liu and G. Ou, *J. Periodontal Res.*, 2018, **53**, 222–231.
208 I. Abrahamsson, N. U. Zitzmann, T. Berglundh, E. Linder, A. Wennerberg and J. Lindhe, *J. Clin. Periodontol.*, 2002, **29**, 448–455.
209 A. Linares, O. Domken, M. Dard and J. Blanco, *J. Clin. Periodontol.*, 2013, **40**, 412–420.
210 L. Guida, A. Oliva, M. A. Basile, M. Giordano, L. Nastri and M. Annunziata, *J. Dent.*, 2013, **41**, 900–907.
211 M. Razali, W. C. Ngeow, R. A. Omar and W. L. Chai, *Biomedicines*, 2021, **9**, 78.
212 Y. Yang, J. Zhou, X. Liu, M. Zheng, J. Yang and J. Tan, *J. Biomed. Mater. Res. B*, 2015, **103**, 116–124.
213 J. P. Albouy, I. Abrahamsson and T. Berglundh, *J. Clin. Periodontol.*, 2012, **39**, 182–187.
214 I. S. Yeo, H. Y. Kim, K. S. Lim and J. S. Han, *Int. J. Artif. Organs*, 2012, **35**, 762–772.
215 H. Herrmann, J. S. Kern, T. Kern, J. Lautensack, G. Conrads and S. Wolfart, *Clin. Oral. Implants Res.*, 2020, **31**, 1094–1104.
216 G. Mainas, V. Ruiz Magaz, C. Valles, J. Mora, J. Candiago, A. Pascual and J. Nart, *Clin. Implant Dent. Relat. Res.*, 2022, **24**, 34–42.
217 J. S. Hermann, D. Buser, R. K. Schenk and D. L. Cochran, *J. Periodontol.*, 2000, **71**, 1412–1424.
218 G. M. Caetano, P. Pauletto, L. A. Mezzomo and E. G. Rivaldo, *Eur. J. Dent.*, 2019, **13**, 497–502.
219 G. Wallner, D. Rieder, M. G. Wichmann and S. M. Heckmann, *Int. J. Oral Maxillofac. Implants*, 2018, **33**, 1119–1125.
220 I. Abrahamsson, T. Berglundh, J. Wennstrom and J. Lindhe, *Clin. Oral. Implants Res.*, 1996, **7**, 212–219.
221 T. Berglundh and J. Lindhe, *J. Clin. Periodontol.*, 1996, **23**, 971–973.
222 N. Esfahanizadeh, S. P. Mirmalek, A. Bahador, H. Daneshparvar, N. Akhoundi and M. Pourhajibagher, *Gen. Dent.*, 2018, **66**, 39–44.
223 P. Ghensi, E. Bettio, D. Maniglio, E. Bonomi, F. Piccoli, S. Gross, P. Caciagli, N. Segata, G. Nollo and F. Tessarolo, *Materials*, 2019, **12**, 2429.
224 Y. Sakamoto, Y. Ayukawa, A. Furuhashi, M. Kamo, J. Ikeda, I. Atsuta, T. Haraguchi and K. Koyano, *Materials*, 2019, **12**, 2748.
225 A. Leong, I. De Kok, D. Mendonca and L. F. Cooper, *Int. J. Oral Maxillofac. Implants*, 2018, **33**, 895–904.
226 R. R. Martins de Barros, M. M. Provinciatti, V. A. Muglia and A. B. Novaes, Jr., *Int. J. Periodont. Restor. Dent.*, 2020, **40**, 73–81.
227 S. Sherif, H. K. Susarla, T. Kapos, D. Munoz, B. M. Chang and R. F. Wright, *J. Prosthodont.*, 2014, **23**, 1–9.
228 D. Bozkaya and S. Müftü, *J. Biomech.*, 2003, **36**, 1649–1658.
229 J. E. Shigley, C. R. Mischke and R. G. Budynas, *Mechanical engineering design*, 7th edn, McGraw-Hill, New York, NY, 2004.
230 L. A. Lang, B. Kang, R. F. Wang and B. R. Lang, *J. Prosthet. Dent.*, 2003, **90**, 539–546.
231 J. H. Bickford, *An Introduction to the Design and Behavior of Bolted Joints, Revised and Expanded*, 3rd edn, CRC Press, New York, NY, 2018.
232 R. S. Cruz, C. A. A. Lemos, V. E. S. de Batista, F. C. Yogui, H. F. F. Oliveira and F. R. Verri, *Int. J. Oral Maxillofac. Surg.*, 2021, **50**, 674–682.
233 X. L. Yu, Y. Chan, L. Zhuang, H. C. Lai, N. P. Lang, W. K. Leung and R. M. Watt, *Clin. Oral. Implants Res.*, 2019, **30**, 760–776.
234 S. K. Mishra, R. Chowdhary and S. Kumari, *J. Clin. Diagn. Res.*, 2017, **11**, ZE10–ZE15.
235 C. Sahin and S. Ayyildiz, *J. Adv. Prosthodont.*, 2014, **6**, 35–38.
236 K. Tsuruta, Y. Ayukawa, T. Matsuzaki, M. Kihara and K. Koyano, *Int. J. Implant Dent.*, 2018, **4**, 11.
237 T. Kitagawa, Y. Tanimoto, M. Odaki, K. Nemoto and M. Aida, *J. Biomed. Mater. Res. B*, 2005, **75**, 457–463.

238 A. C. Dayrell, P. Y. Noritomi, J. M. Takahashi, R. L. Consani, M. F. Mesquita and M. B. dos Santos, *Int. J. Prosthodont.*, 2015, **28**, 621–623.
239 J. Markose, S. Eshwar, S. Srinivas and V. Jain, *Clin. Implant Dent. Relat. Res.*, 2018, **20**, 646–652.
240 T. Koutouzis, G. Koutouzis, H. Gadalla and R. Neiva, *Int. J. Oral Maxillofac. Implants*, 2013, **28**, 807–814.
241 K. X. Michalakis, P. L. Calvani, S. Muftu, A. Pissiotis and H. Hirayama, *J. Oral Implantol.*, 2014, **40**, 146–152.
242 F. Saleh Saber, N. Abolfazli, S. J. Ataei, M. T. Motlagh and V. Gharekhani, *J. Dent. Res. Dent. Clin. Dent. Prospects*, 2017, **11**, 110–116.
243 M. Khalili, A. Luke, H. El-Hammali, L. DiPede and S. Weiner, *Int. J. Oral Maxillofac. Implants*, 2019, **34**, 1084–1090.
244 N. P. Lang and H. Loe, *J. Periodontol.*, 1972, **43**, 623–627.
245 T. Albrektsson, G. Zarb, P. Worthington and A. R. Eriksson, *Int. J. Oral Maxillofac. Implants*, 1986, **1**, 11–25.
246 R. M. Palmer, P. J. Palmer and B. J. Smith, *Clin. Oral. Implants Res.*, 2000, **11**, 179–182.
247 L. Puchades-Roman, R. M. Palmer, P. J. Palmer, L. C. Howe, M. Ide and R. F. Wilson, *Clin. Implant Dent. Relat. Res.*, 2000, **2**, 78–84.
248 E. Schiegnitz, R. Noelken, M. Moergel, M. Berres and W. Wagner, *Clin. Oral. Implants Res.*, 2017, **28**, 721–726.
249 J. Hadzik, M. Krawiec, P. Kubasiewicz-Ross, A. Prylinska-Czyzewska, T. Gedrange and M. Dominiak, *Med. Sci. Monit.*, 2018, **24**, 5645–5652.
250 R. Caricasulo, L. Malchiodi, P. Ghensi, G. Fantozzi and A. Cucchi, *Clin. Implant Dent. Relat. Res.*, 2018, **20**, 653–664.
251 R. S. Pessoa, R. M. Sousa, L. M. Pereira, F. D. Neves, F. J. Bezerra, S. V. Jaecques, J. V. Sloten, M. Quirynen, W. Teughels and R. Spin-Neto, *Clin. Implant Dent. Relat. Res.*, 2017, **19**, 97–110.
252 E. Kononen, M. Gursoy and U. K. Gursoy, *J. Clin. Med.*, 2019, **8**, 1135.
253 A. Ispas, C. M. Mihu, A. M. Craciun and M. Constantiniuc, *Rom. J. Morphol. Embryol.*, 2018, **59**, 211–217.
254 T. K. Pilgram, C. F. Hildebolt, N. Yokoyama-Crothers, M. Dotson, S. C. Cohen, J. F. Hauser and E. Kardaris, *J. Periodontol.*, 1999, **70**, 829–833.
255 H. Y. Kim, J. Y. Yang, B. Y. Chung, J. C. Kim and I. S. Yeo, *J. Periodontal. Implant Sci.*, 2013, **43**, 58–63.
256 B. E. Pjetursson and K. Heimisdottir, *Eur. J. Oral Sci.*, 2018, **126**(Suppl 1), 81–87.
257 P. Simonis, T. Dufour and H. Tenenbaum, *Clin. Oral. Implants Res.*, 2010, **21**, 772–777.
258 T. Jemt, *Int. J. Prosthodont.*, 2018, **31**, 531–539.
259 T. Jemt, *Int. J. Prosthodont.*, 2018, **31**, 425–435.
260 T. Jemt, *Int. J. Prosthodont.*, 2019, **32**, 36–44.
261 T. Jemt, *Int. J. Prosthodont.*, 2019, **32**, 143–152.
262 L. Laurell and D. Lundgren, *Clin. Implant Dent. Relat. Res.*, 2011, **13**, 19–28.
263 X. Ren, H. C. van der Mei, Y. Ren and H. J. Busscher, *Acta Biomater.*, 2019, **96**, 237–246.
264 L. G. de Vasconcellos, A. N. Kojima, R. S. Nishioka, L. M. de Vasconcellos and I. Balducci, *J. Oral Implantol.*, 2015, **41**, 149–154.
265 N. Palacios-Garzón, R. Ayuso-Montero, E. Jané-Salas, J. M. Anglada-Cantarell and J. López-López, *Coatings*, 2020, **10**, 1044.